University of Illinois at Urbana-Champaign

ACRC

Air Conditioning and Refrigeration Center A National Science Foundation/University Cooperative Research Center

Dual Evaporator Household Refrigerator Performance Testing and Simulation

D. W. Gerlach and T. A. Newell

ACRC CR-40 March 2001

For additional information:

Air Conditioning and Refrigeration Center
University of Illinois
Mechanical & Industrial Engineering Dept.
1206 West Green Street
Urbana, IL 61801

(217) 333-3115

The Air Conditioning and Refrigeration Center was founded in 1988 with a grant from the estate of Richard W. Kritzer, the founder of Peerless of America Inc. A State of Illinois Technology Challenge Grant helped build the laboratory facilities. The ACRC receives continuing support from the Richard W. Kritzer Endowment and the National Science Foundation. The following organizations have also become sponsors of the Center.

Amana Refrigeration, Inc.
Arçelik A. S.
Brazeway, Inc.
Carrier Corporation
Copeland Corporation
Dacor
Daikin Industries, Ltd.
DaimlerChrysler Corporation
Delphi Harrison Thermal Systems
Frigidaire Company
General Electric Company
General Motors Corporation
Hill PHOENIX
Honeywell, Inc.
Hussmann Corporation
Hydro Aluminum Adrian, Inc.
Indiana Tube Corporation
Invensys Climate Controls
Kelon Electrical Holdings Co., Ltd.
Lennox International, Inc.
LG Electronics, Inc.
Modine Manufacturing Co.
Parker Hannifin Corporation
Peerless of America, Inc.
Samsung Electronics Co., Ltd.
Tecumseh Products Company
The Trane Company
Thermo King Corporation
Valeo, Inc.
Visteon Automotive Systems
Wolverine Tube, Inc.
York International, Inc.

For additional information:

Air Conditioning & Refrigeration Center
Mechanical & Industrial Engineering Dept.
University of Illinois
1206 West Green Street
Urbana, IL 61801

217 333 3115

Abstract

The performance of dual evaporator household refrigerators was studied experimentally and by numerical simulation. This study considers only serial connection where the refrigerant flows through the fresh food evaporator and then through the freezer evaporator without a pressure drop between the evaporators. The prototype tested had insufficient compressor power and a higher cabinet thermal conductance than designed. In addition, the exit of the freezer evaporator was always two-phase affecting compressor performance. However, control of the fresh food cabinet air temperature was achieved through turning the fan off and on during operation. This fan cycling affected both the performance of the prototype and the charge distribution inside the system. The data from the tests was used to check the accuracy of a numerical model of dual evaporator refrigerators. It was shown that the accuracy of the model could be improved through various adjustments. However, uncertainty about the compressor performance limited the accuracy to between 10 and 20 percent. This model was then used to simulate the performance of the refrigerator as originally designed and with larger and smaller evaporators. In general, charge requirements increased with evaporator size as did the system's sensitivity to ambient temperature. Increasing the fresh food evaporator size did not significantly increase COP but did increase capacity.

Table of Contents

List of Figures

Chapter 1: Introduction

1.1 Overview

Household refrigerator manufacturers are currently very interested in dual evaporator refrigerators. These refrigerators may regulate cabinet humidity better than traditional refrigerator designs and have the potential of greater efficiency.

In American-style auto-defrost combination refrigerator-freezers, air is blown over a single evaporator to both compartments. Dual evaporator designs have separate evaporators for the fresh food and freezer compartments and no airflow between the compartments.

This study is an investigation of the basic performance parameters and behavior of a dual evaporator refrigerator. Although various configurations for the refrigerant circuitry have been proposed, this study considers only serial connection where the refrigerant flows through the fresh food evaporator and then through the freezer evaporator.

Performance tests were conducted using a prototype refrigerator. This same design was simulated numerically and the simulation results were compared to the experimental results. The numerical simulation was then used to predict the performance of the refrigerator with changes in the evaporator sizes and other design parameters.

1.2 Potential Advantages of Dual Evaporator Design

Dual evaporator refrigerators may be more thermodynamically efficient than standard refrigerators, depending on the refrigerant circuit design. In single evaporator refrigerator-freezers, the evaporator temperature must be colder than the freezer. A dual evaporator refrigerator can be designed so that the pressure and temperatures in the evaporators are controlled separately. This allows the fresh food evaporator to more closely match the air temperature, thus reducing the irreversibilities associated with the heat transfer. Also, the evaporators can be fed by separate capillary tubes or even separate compressors that are optimized for each compartment.

The second major advantage of the dual evaporator system is humidity control. In a single evaporator system, humid air from the fresh food compartment comes in contact with the very cold evaporator, causing frost growth. The dehumidified air is then returned to the fresh food cabinet. This dry air, in turn, desiccates the food and reduces food quality. If the fresh food evaporator more closely matches the air temperature in the fresh food compartment it will dehumidify the air less and build up less frost. This decreases the need for defrosting with a heater and increases energy efficiency.

The refrigerators tested in this study do not have a theoretical improvement in efficiency as they were run with the two evaporators at approximately the same temperature and pressure. However, they do have the advantage of better humidity control and are a useful first step towards investigating more advanced systems.

1.3 Prior Work

Dual evaporator refrigerator-freezers have been investigated in both academia and industry. In addition, several companies have produced household dual evaporator refrigerators.

During the 1970's and 1980's Amana Refrigeration, Inc. produced dual evaporator refrigerators with the evaporators connected in series. The fresh food evaporator used free convection. The freezer evaporator used free convection in the manual defrost model and forced convection in the auto defrost model. The manual defrost model consumed 50 kWh per month, while the auto defrost model consumed 75 kWh. These values were considerably better than comparably sized models of the day. Because the humid fresh food air did not come in contact with the freezer evaporator, less frost formed on it. One owner recalls that the defrost frequency for the manual defrost model could be as low as once or twice a year if the freezer was opened infrequently (Bullard (2000)). An advanced version of this refrigerator was developed for an U.S. Department of Energy study on high efficiency automatic defrosting refrigerator-freezers (Topping (1981) and Bohman (1982)).

Samsung currently manufactures a dual evaporator system that it calls a "twin cooling system." The system uses a single compressor. Although information on the refrigerant circuit was unavailable, Samsung claims increased energy efficiency because of the separation of airflows and decreased defrost heater use. According to Samsung, this system maintains better food quality as a result of higher fresh food humidity, faster compartment temperature pull down, and the separation of fresh food and freezer odors (Samsung (2000)).

In addition, Samsung engineers published a paper discussing the operation of a dual evaporator refrigerator (Lee (1996)). However, it is not clear whether this system is the same as the one put into production. The paper describes a system with the fresh food and freezer evaporators in series. In this system, the freezer and fresh food fans operate independently. When the compressor turns on due to high cabinet temperatures, both fans generally turn on. The fans then turn off independently when they have reduced the temperature in their respective compartments below the set point. When both compartments are cooled, the compressor shuts off. During parts of the compressor off time, the fresh food fan runs to defrost the evaporator and make use of the cooling capacity of the refrigerant remaining in the evaporator. Fresh food humidity is also improved in this system.

Lavanis et al. (1998) tested a refrigerator that used an alternating evaporator duty cycle. This design had a single compressor, condenser, and suction line heat exchanger unit. A solenoid valve then directed the refrigerant flow to either the freezer or fresh food evaporator. Each evaporator had a separate expansion device. In the same study Lavanis also tested a dual evaporator system with the evaporators connected in series. The alternating evaporator duty cycle was found to have an 8.5% efficiency improvement over the series cycle. This was mainly a result of the lower evaporation pressure during the fresh food part of the cycle.

Won et al. (1994) tested a dual loop evaporator system with two compressors and completely separate circuits for each compartment. A 3.5% improvement in energy efficiency was observed. In such a system, the compressors are smaller and less efficient. This reduces the energy gained from optimizing separate circuits for each compartment. Bare (1992b) used computer simulations to select the best refrigerants for this type of cycle. Energy efficiency, safety, environmental impact, and cost were considered as criteria. Of the refrigerants studied, R-152a was best for the freezer and R-152a and R-142b were best for the fresh food cabinet.

Kim et al.(1995a and 1995b) studied dual evaporator refrigerator they called a "tandem system." The refrigerant exits the condenser and flows through a suction line heat exchanger. It then passes through a tube in thermal contact with the fresh food evaporator. Next, the refrigerant flows through an expansion device, into the

freezer evaporator, and through the fresh food evaporator. The fresh food and freezer evaporator fans never operate simultaneously. Consequently, the fresh food evaporator acts as an intercooler when its fan is off. This system achieves an 18% energy savings over a similar ordinary single evaporator system, primarily by reducing and controlling charge migration during the compressor off cycle.

Several patents have been filed by the General Electric Company on household refrigerator/freezer systems with two evaporators (Jaster (1990a) and (1990b) and Day (1993)). Each of these designs has a phase separator between the evaporators. In two of the patents, the refrigerant flows through an expansion valve and then into the fresh food evaporator (Jaster (1990a) and (1990b)). The liquid refrigerant is then separated from the vapor and sent through a second expansion valve and into the freezer evaporator. One design uses a two-stage compressor and the other two compressors in series. The vapor drawn off from the phase separator is sent to the middle of the two-stage system or in between the two compressors in the other system. These patents make use of the phase separator as an intercooler. The third patent uses a valve so that the refrigerant returning to the compressor is drawn from the freezer evaporator outlet or the vapor from the phase separator (Day (1993)).

A number of studies dealing with dual evaporator refrigerators were funded by a U.S. Environmental Protection Agency initiative on zeotropic refrigerant mixtures. Zeotropes (also called non-azeotropes) change phase over a temperature range because of the difference in volatility of the refrigerants in the mixtures. This is well suited to exchanging heat with reservoirs at different temperatures, such as the two compartments in a refrigerator. Such a system is called a Lorenz-Meutzner cycle. Most of these studies reported a theoretical improvement in COP due to a lower temperature difference between the air and the refrigerant (Jung (1991)). However, this improvement is dependent on whether the air temperature is held constant or changes as it passes over the evaporator (Smith (1990 and 1994)). Actual testing of dual evaporator refrigerators with zeotropic refrigerant mixtures showed modest improvements in efficiency over single component refrigerant systems (Rose (1992) and Smith (1990 and 1994)). Independent control of the refrigerator and freezer temperatures was achieved by switching refrigerant flow from passing through both evaporators to passing through only one evaporator. However, this control scheme increased power consumption (Simmons (1996)). An overview of some of the EPA funded work on zeotropic refrigerant mixtures is found in Bare (1992a).

1.4 Conclusion

This study includes experimental work with dual evaporator refrigerators as was previously done in a number of studies. However, it also includes the development and validation of a complex computer model of the serial evaporator configuration. This aspect has not been well documented in the open literature and contributes to the future development of production dual evaporator refrigerators.

Chapter 2: Dual Evaporator Performance Tests

2.1 Introduction

Energy performance tests were conducted to determine the coefficient of performance (COP) of a dual evaporator refrigerator prototype. Two prototype dual evaporator refrigerators were used for performance testing. They were specially built for this research and therefore differ slightly from a production model. They are described below.

Reverse heat leak tests were performed to determine the cabinet heat gain characteristics. A series of tests were run to determine an optimal value for the refrigerant charge. After the optimal charge was determined, more tests were conducted to gauge the effect of different refrigerator control schemes on performance.

2.2 Prototype Description

The refrigerators tested are similar to standard top-mount household refrigerator freezers. A diagram of the cabinet interior is shown in Figure 2.2.1.

The order of components in the refrigerant circuit is shown in Figure 2.2.2. The prototypes were constructed with bypass valves and needle valves. When the bypass valves are closed, the pressure drops between system components are changed by adjusting the needle valves. The refrigerant circuit was attached to the outside of the cabinet (Figure 2.2.3) to allow easy access for instrumentation and adjustment.

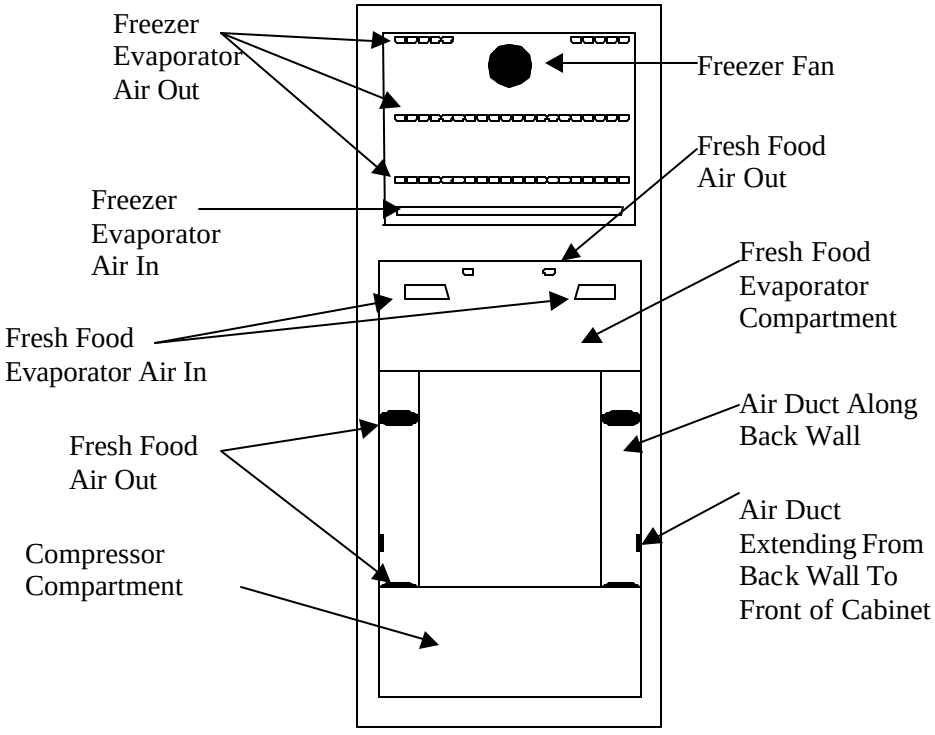

Figure 2.2.1 Cabinet Interior With Air Distribution System

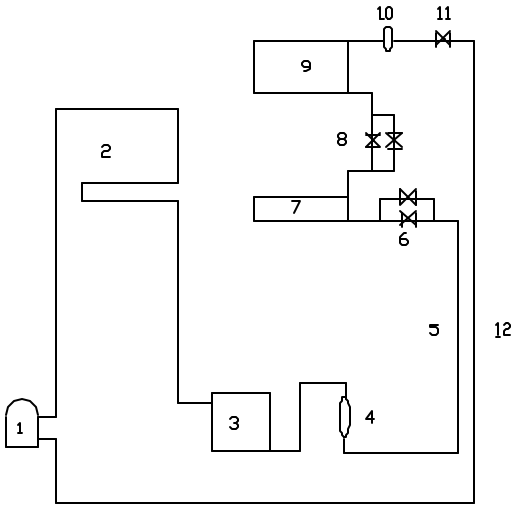

1. Compressor
2. Hot Loop/Flange Heater
3. Condenser
4. Filter Dryer
5. Capillary Tube Part of Internal Heat Exchanger
6. Bypass Valve and Needle Valve
7. Fresh Food Evaporator
8. Bypass Valve and Needle Valve
9. Freezer Evaporator
10. Accumulator
11. Cutoff Valve
12. Suction Line Part of Internal Heat Exchanger

Figure 2.2.2 Refrigerant Circuit Schematic

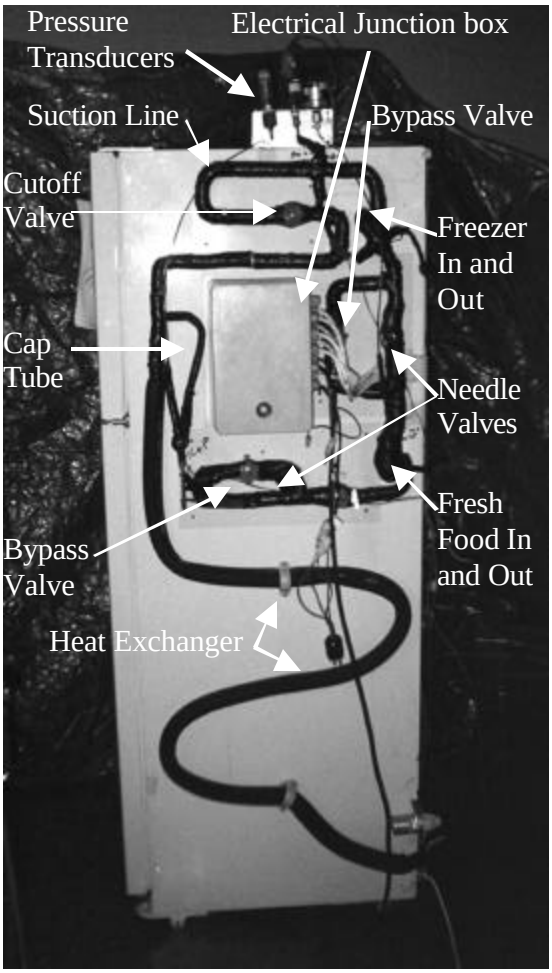

Figure 2.2.3 Refrigerant Circuit on Cabinet Exterior

The fans and defrost heaters were connected to screw terminals in a junction box on the side of the refrigerator. The compressor was separately connected to a standard AC plug. The separate wiring and lack of an installed controller allowed separate measurement of each component's power and the use of different control schemes.

2.3 Reverse Heat Leak Tests

The thermal conductance or overall heat transfer coefficient (UA) of the refrigerator cabinet must be measured in order to calculate the heat entering the refrigerator from its environment. The UA is a constant that is multiplied by the temperature difference between the inside and outside of the cabinet to obtain the steady state heat flow between the cabinet interior and the environment:

$$Q=UA*(T_{ambient}-T_{interior})$$

This value includes the conductance of the refrigerator wall, the convection heat transfer coefficients on the inside wall of the cabinet and on the outside of the refrigerator, and any losses due to air leakage through the door seal and other cabinet penetration points.

The UAs were determined by reverse heat leak tests as described below. Because the refrigerator has two separate compartments, it was necessary to determine the UA of the fresh food and freezer compartments with respect to the outside and the UA of the mullion between the two compartments.

2.3.1 Experimental Setup

Heat leak tests were run twice on the first prototype. Thermocouples were installed differently for the two test series. For the first series, thermocouples were placed in the fresh food cabinet so that there were pairs at the top, middle, and bottom of the cabinet. Five thermocouples were placed in the freezer so that there were two at the top and bottom and one in the exact center of the compartment. The second set of tests was run to confirm the earlier results and was run while the refrigerator was fully instrumented as described in Appendix A. Heat leak tests on the second prototype were performed using air thermocouples arranged the same as for the first prototype during the second test series.

Electrical resistance heaters were made of nichrome wire strung between ceramic spacers attached to a wood frame (Figure 2.3.1.1). They were placed in each compartment. For the first prototype, the freezer heater resistance was 93 ohms and the freshfood compartment heater resistance was 200 ohms. For the second prototype, the heaters were 79 ohms and 196 ohms respectively. Variable transformers, called variacs, were used to control the voltage supplied to the heaters. Watt transducers measured the power of the heaters and evaporator fans.

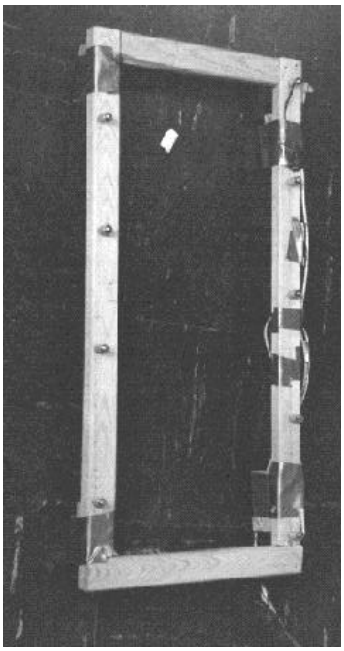

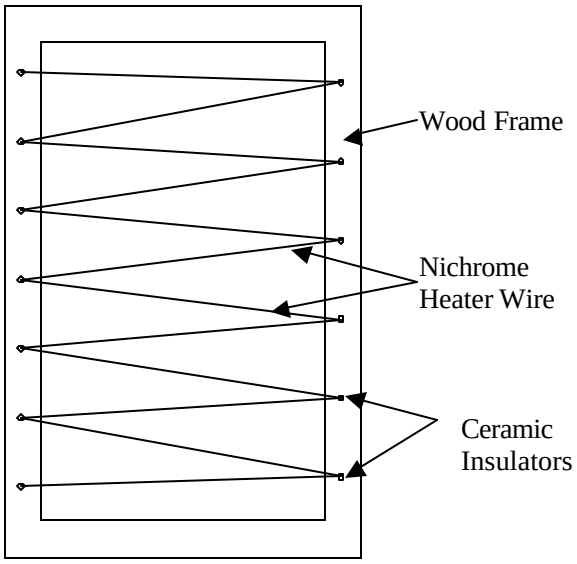

Figure 2.3.1.1 Photo of Cabinet Heater (left), Diagram of Cabinet Heater (right)

All tests were run in the temperature controlled test chamber and using the data acquisition system described in Appendix A.

2.3.2 Experimental Procedure

The refrigerator was placed in the temperature controlled test chamber. The fan in each compartment was turned on to prevent thermal stratification and the voltage to each heater was selected using the variacs. The refrigerator was left undisturbed until it had reached thermal equilibrium and the interior temperatures had reached a steady state condition. This typically took 18 to 24 hours. The temperatures of the chamber and inside the refrigerator compartments were measured every minute so that the approach to equilibrium could be monitored.

2.3.3 UA Calculation Procedure

The reverse heat leak tests were designed to determine three variables (UA freezer, UA mullion, and UA fresh food). The energy balances for the compartments were calculated as:

$$0=UA_{freezer}(T_{amb}-T_{freezer})+UA_{mullion}(T_{freshfood}-T_{freezer})+Q_{freezer}$$

$$0=UA_{freezer}(T_{amb}-T_{freshfood})+UA_{mullion}(T_{freezer}-T_{freshfood})+Q_{freshfood}$$

In principle, these values should always equal zero. Therefore, three tests with different combinations of ambient, freezer, and fresh food temperatures should generate a system of three simultaneous equations. In practice, experimental error required that more than three tests be run. Consequently, the system of equations is over specified.

To remedy this, the UAs were initially guessed using the predicted design values. However, experimental error causes some level of energy imbalance. Energy imbalances for each test were calculated and then squared. The squared deviations from zero were then summed. The solver function of Microsoft Excel was used to minimize this value by changing the guessed UA values. The UAs were constrained to be positive numbers.

2.3.4 Results

The UA between the fresh food compartment and the ambient for the first prototype was measured as 1.90 watts/°C. The freezer to ambient UA was 0.99 watts/°C. The mullion UA was 0.27 watts/°C. For the second prototype, they were measured as 2.09, 0.73, and 0.13 watts/°C for the fresh food, freezer, and mullion UAs.

These UA values are higher than the expected design values. The design values assumed that the polyurethane foam insulation had the same thermal conductivity as that of production models. However, these prototypes were hand built and the insulation may not have filled the wall cavities as well as expected. Also the refrigerant circuiting penetrated the cabinet walls at several locations in order to allow manual control of refrigerant flow conditions. The cabinet penetrations allowed heat transfer out of the cabinet by conduction along the tubing and air leakage. The possibility of a thermal siphon effect with the refrigerant flowing into and out of the cabinet due to free convection was considered. However, a heat leak test with the tubing evacuated showed no difference from results with the system charged. Therefore, whatever caused the increased UAs was not caused by the refrigerant.

2.4 Performance Test Procedures

All the performance tests were conducted in the ACRC (Air Conditioning and Refrigeration Center at the University of Illinois) temperature controlled test chamber (See Hamm (1994) for a description of the chamber as originally built). The nominal values of the ambient temperature during each test series were 16, 25, 32, and 43 °C. The test chamber adequately held these values for each temperature level except the 43 °C tests. This temperature exceeded the maximum that the test chamber could hold steady. Consequently, the 43 °C level was only used on the earlier tests and then abandoned.

Before charging the refrigerator, a vacuum pump evacuated the system for approximately one hour. The refrigerant tank was placed on the charging scale and the hose connected to the charging valve. A two-way valve with a hand wheel was used instead of the typical Schrader valve. The hose was connected from the tank to the charging valve. The hose was filled with refrigerant and the air inside it was expelled by slightly loosening and retightening the connection to the charging valve. Then the hose was secured with tape so that it would not move during charging. The weight of the tank was read and recorded. Then the charging valve was opened. This sucked part of the charge into the system. In order to drive the complete charge into the system, either the tank was heated with a heat gun or the refrigerator compressor was operated. When sufficient charge had entered the system, the charging valve was closed.

The main source of error in this method is the refrigerant hose. During charging, part of its weight is supported by the refrigerator and part by the scale. If the hose moves or shifts during charging the weight reading on the scale changes. Visual observation confirmed that the hose did not move during charging. In addition, the mass of the refrigerant in the hose may change over the course of charging. The maximum change in the charge would be if the hose was completely full of liquid which changed completely to vapor. This was unlikely as the tank was positioned so that the refrigerant entering it was single phase. However, such an unlikely change at 25°C could cause an error of 36 grams. Another possibility is that the mass in the charging hose could change due to temperature change from the heat gun. A rise in temperature from 25°C to 75°C at a quality of 1 would cause an

error of 3 grams. The same temperature change at a quality of 0 would cause an error of 7.5 grams. A realistic estimate of the charging error would be in the range of 10-15 grams or 3-6%.

After the refrigerator was charged, it was connected to the data acquisition system. The compressor and other components were plugged into watt transducers as described in Appendix A. No heaters were used in the cabinet to produce artificial loads as is sometimes done in refrigerator testing to prevent cycling and ensure steady state operation (Srichai (1997)).

The compressor and freezer fans ran continuously during all tests. Because the compressor was underpowered and the cabinet thermal conductance was higher than the design value, the compressor was not cycled. Even at 100% run time it did not adequately cool the cabinet. The fresh food fan was switched on and off to control the fresh food temperature as described below. System temperatures and pressures were measured every minute throughout the tests. The power consumptions of the compressor and evaporator fans were measured separately. Continuous data logging allowed system equilibrium cycling conditions to be determined. This usually took 3-5 hours when changing from one ambient temperature to another. However, to ensure repeatable cycling performance, the system was run continuously anywhere from 10 to 48 hours.

2.5 Fresh Food Temperature Control

A controller (Omega CN9121) turned the fresh food fan evaporator off and on to regulate the temperature of the fresh food compartment. The controller was connected to a thermocouple placed inside of a 0.5 inch diameter brass slug and suspended in the center of the fresh food cabinet. The brass slug was intended to time average the air temperature due to its thermal mass. This would reduce the effect of small air currents inside the fresh food compartment on the controller. The set point of the controller was set at 3 °C. In addition to the hysteresis introduced by the brass slug, the controller was programmed to turn on at 3.8 °C and off at 2.8 °C. The on-off cycle of the fan was influenced by the ambient temperature but was on the order of tens of minutes (Figure 2.5.1).

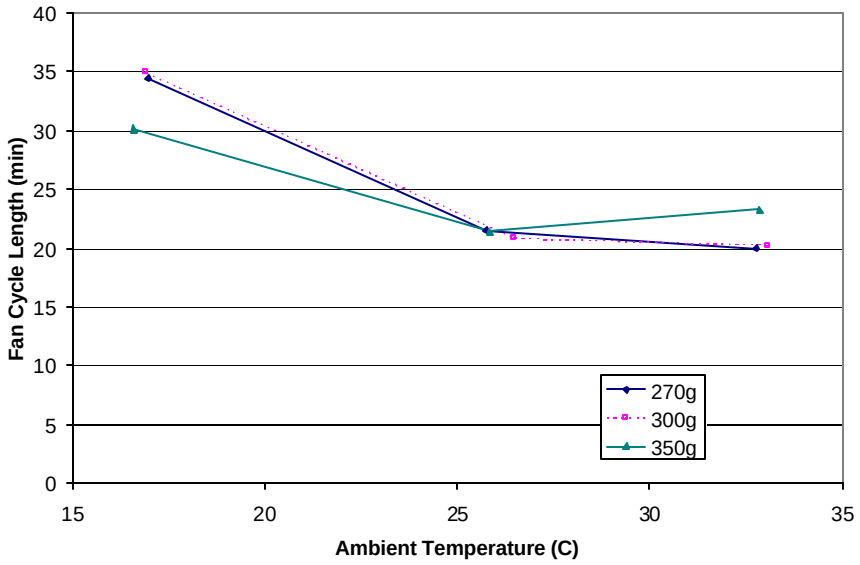

Figure 2.5.1 Variation in Fresh Food Fan Cycle Period with Ambient Temperature During Long Fan Cycle Tests

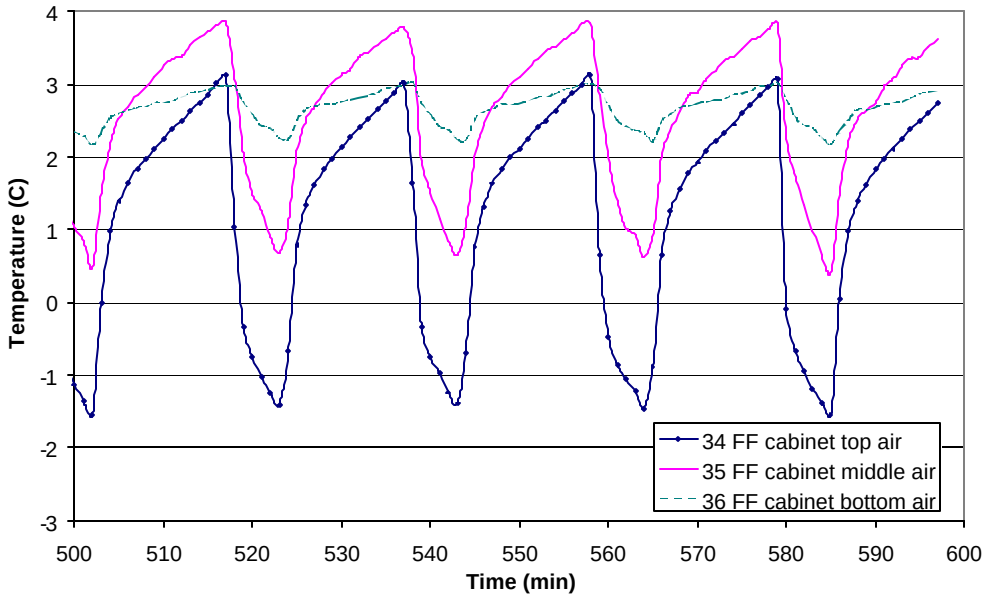

Figure 2.5.2 Variation in Fresh Food Cabinet Air Temperatures (300g Charge 25°C Ambient)

The fresh food compartment's temperature remained within an appropriate range (Figure 2.5.2). The freezer air temperatures also oscillated due to the fresh food fan cycling (Figure 2.5.3). Because the prototype's thermal conductance was higher than the design value, even at 100% compressor run time the freezer compartment was warmer than the target maximum of –18 °C during the 32 °C ambient tests.

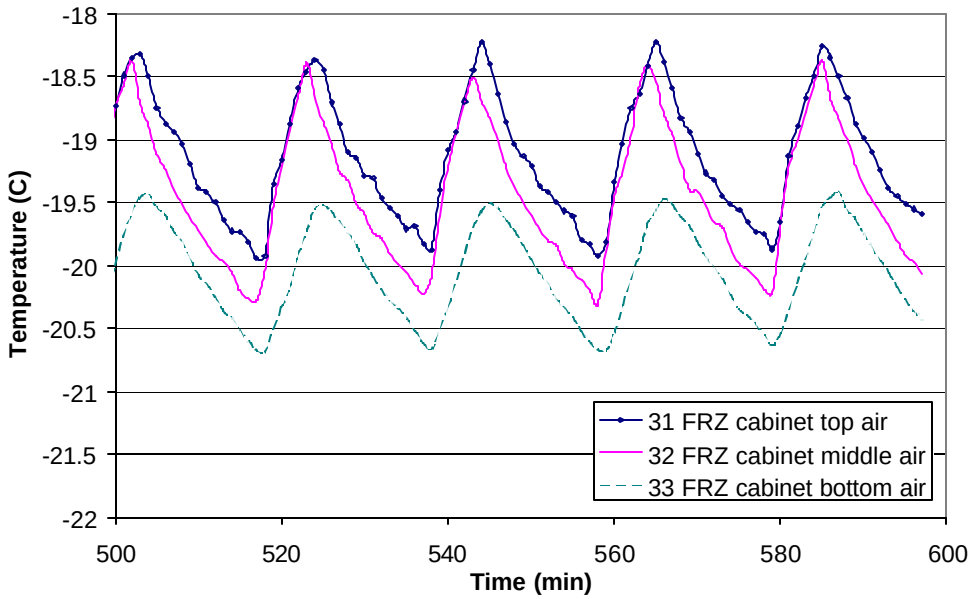

Figure 2.5.3 Variation in Freezer Cabinet Air Temperatures (300g Charge 25°C Ambient)

The effect of the fan cycle length on the refrigerator performance was studied by changing the fresh food fan control scheme. To achieve a more steady state operation, the length of the fresh food fan cycle was reduced to about one minute. Again, the cycle length depends on the ambient temperature (Figure 2.5.4). However, the cold airflow from the fresh food evaporator requires a period of time from fan startup to reach the center of the fresh food compartment (see Inan (1999) for more detail on the airflows in this refrigerator.). This response time plus the inherent hysteresis in the brass slug positioned in the center of the fresh food compartment was longer than the target cycle length. Consequently, the fan controller was connected to the air thermocouple in the meat drawer. Because the meat drawer was cooler than the center of the refrigerator, the controller turned the fan off earlier when the thermocouple was placed in the meat drawer, as compared to the long cycle test when the controller was in the center of the fresh food compartment. This led to a higher average temperature in the compartments. To compensate for this higher temperature the controller set point was reduced to 1.5 °C. The on and off points were set 0.6 °C above and below this value.

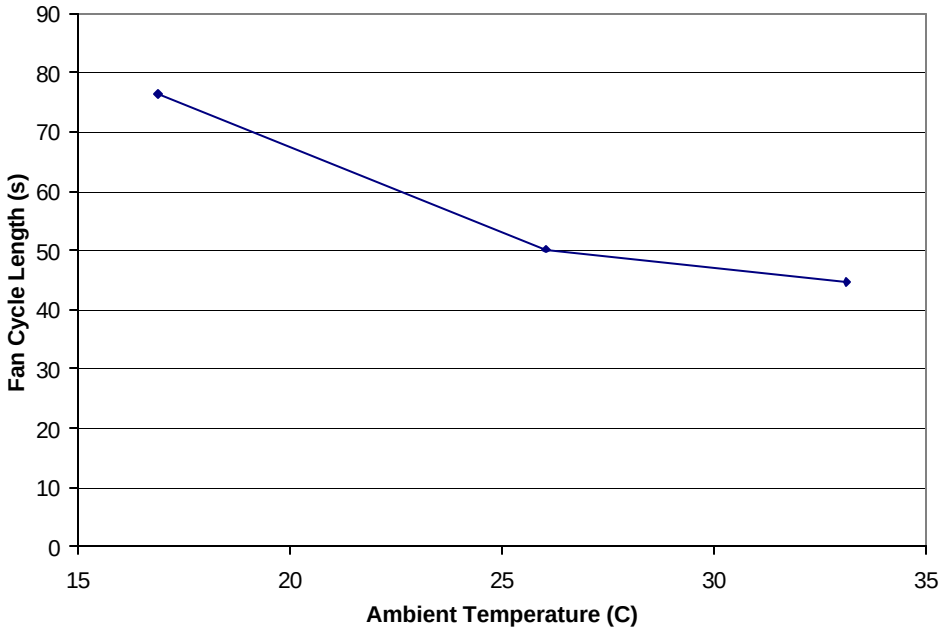

Figure 2.5.4 Variation in Fresh Food Fan Cycle Period with Ambient Temperature During Short Fan Cycle Tests

Because the fan cycle time was on the same order as the sampling time, the fresh food fan power could not be determined by sampling at one minute intervals. Consequently, the fan power was measured separately. After the data for all the other measurements was collected, the refrigerator was allowed to continue operating at steady state. The fan power was measured every second for at least 10 minutes. The average fan power over the last 10 minutes was used.

2.6 Charge Determination Tests

In order to determine a good mass for the refrigerant charge, a performance test series was run with 270, 300, and 350-gram charges of R134a. The COP rose when increasing the charge from 270g to 300g. However, it dropped off sharply at 300g (Figure 2.7.1.1). The 300g charge was selected as the best charge for future tests.

2.7 Results and Analysis

2.7.1 COP Increase with Rising Ambient Temperature

The COP rises with an increase in ambient temperature in all the test series (see Figures 2.7.1.1 and 2.7.1.2). Because the insulation was less than the design value, the freezer temperature increased with an increase in ambient temperature (see Figure 2.7.1.3). The temperature of the refrigerant in the freezer follows the freezer air temperature and stays about 3-5 °C below it. As a result, the freezer saturation pressure increases with increasing ambient temperature. The compressor efficiency increases with increasing inlet pressure. Of course, increasing ambient temperature places a larger cooling load on the refrigerator because the conduction heat transfer to the fresh food compartment increases as does the fresh food fan on-time fraction. Therefore, the condensing temperature increases (Figure 2.7.1.4). This should decrease compressor efficiency by increasing its exit pressure. However, compressor efficiency is more sensitive to low side temperatures than to high side temperatures in the region of the modified compressor map (see Section 3.5.1 for discussion of the compressor map modifications) in which the test refrigerator operated (Figure 2.7.1.5).

The effects of the variable freezer temperature mask other effects and cause the test refrigerator to perform differently than a production refrigerator with a controlled freezer temperature. If the freezer temperature could be held steady at the desired value, then the evaporating pressure and temperature would not be as strong a function of the ambient temperature. Consequently, COP would be a less strong function of the ambient temperature. In addition, the compressor would need to be cycled on and off, or heaters would need to be added to the compartments to make the refrigerator operate continuously during testing.

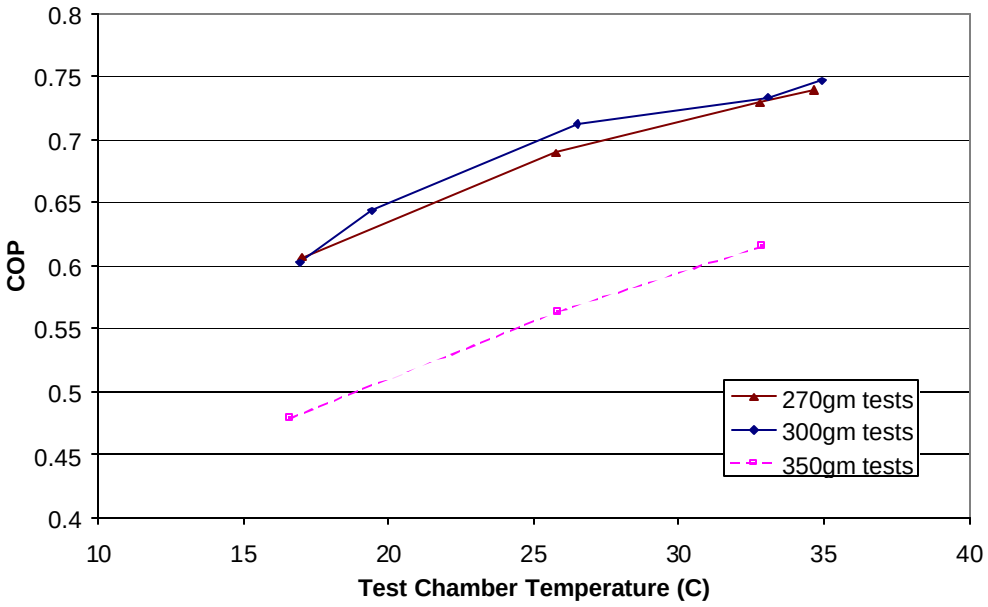

Figure 2.7.1.1 COP versus Ambient Temperature for Charge Optimization Tests

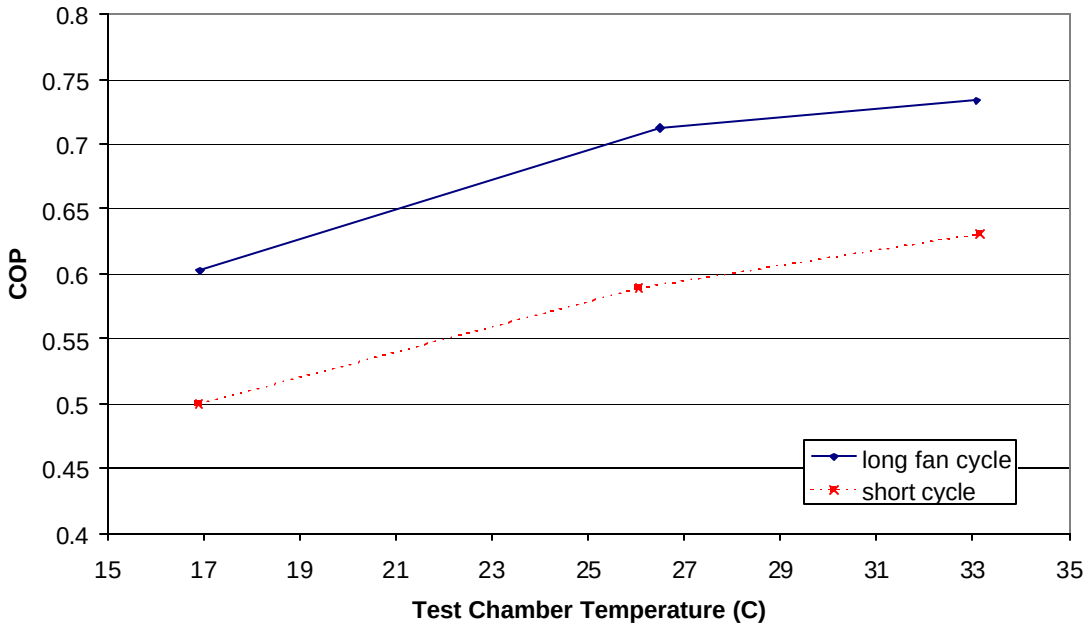

Figure 2.7.1.2 COP Versus Ambient for Long and Short Fan Cycle Tests

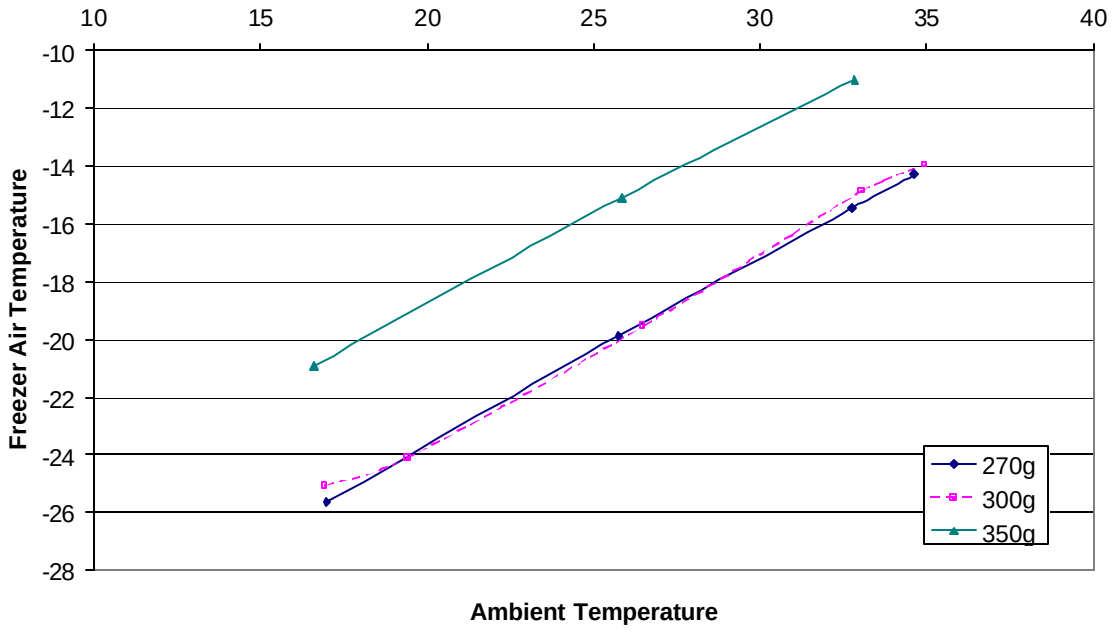

Figure 2.7.1.3 Freezer Air Temperature versus Ambient Temperature

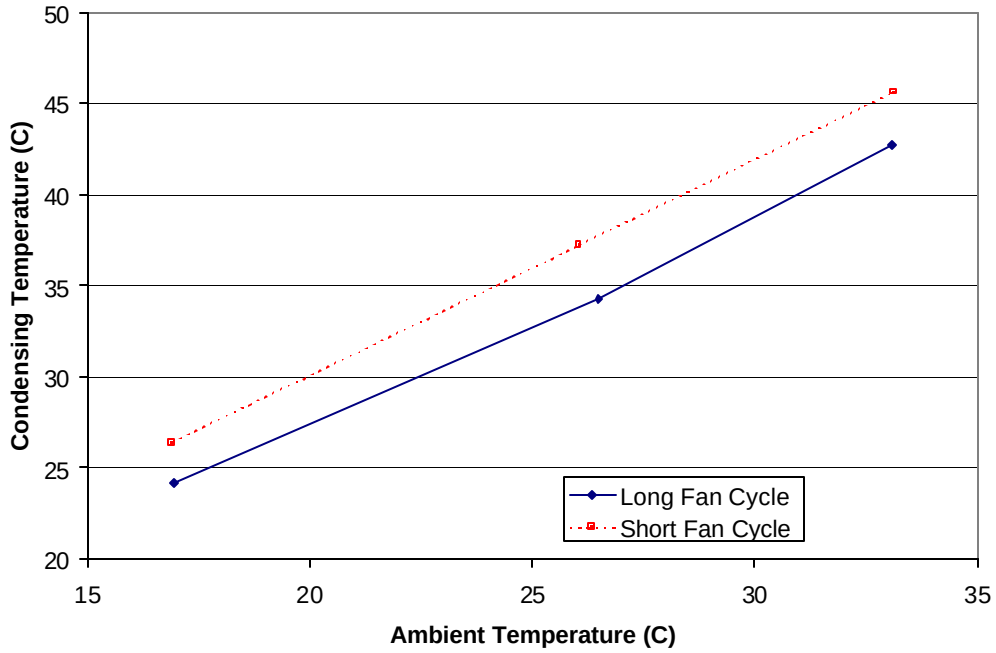

Figure 2.7.1.4 Condensing Temperature versus Ambient Temperature

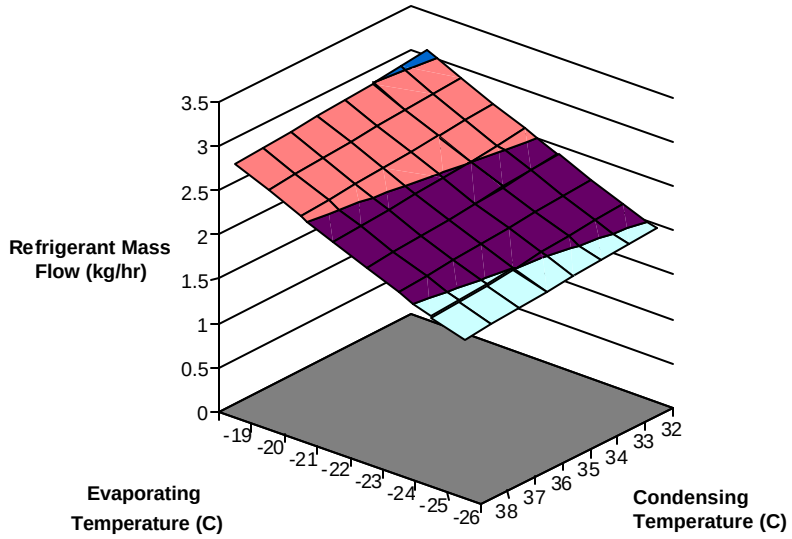

Figure 2.7.1.5 Compressor Mass Flow Map

2.7.2 Effects of Fresh Food Fan Cycling on Performance and Charge Distribution

The refrigerant appears to shift into and out of the fresh food evaporator due to the fan cycling. While the fan is off the charge builds up in the evaporator and a two phase mixture exits the fresh food evaporator. However, the liquid phase preferentially remains in the evaporator while the vapor phase passes through to the freezer. Consequently, the quality in the fresh food evaporator decreases during the fan off cycle and the charge in the fresh food builds up with time. When the fan turns on, a large portion of the evaporator tubing is wetted, causing a high initial heat transfer coefficient (Figure 2.6.2.1). As the accumulated charge begins to boil off, the wetted surface area decreases and the overall heat transfer rate decays.

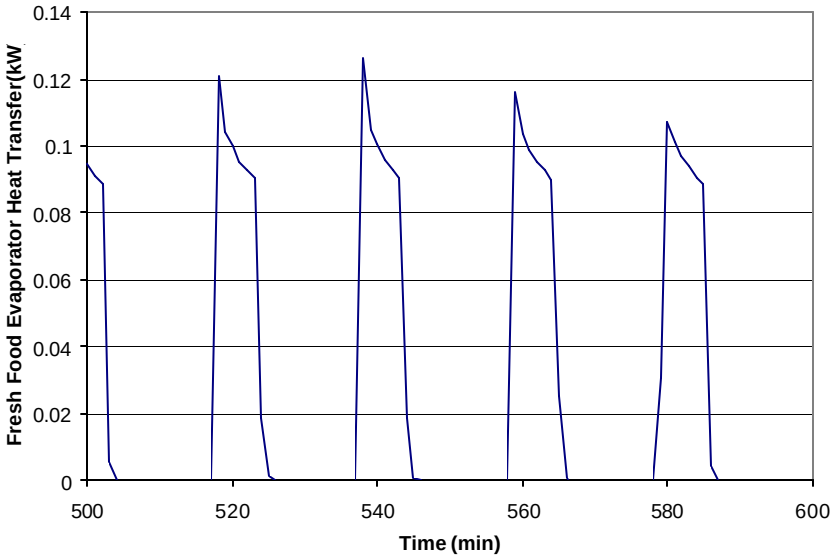

Figure 2.7.2.1 Heat Transfer Across Fresh Food Evaporator

The freezer evaporator exit appears to always be two-phase. Figure 2.7.2.2 shows the temperature (FRZ evap out) of the refrigerant measured by the immersion thermocouple after the accumulator and at the entrance to the suction line. The saturation temperature as determined by the pressure transducer at the same location is labeled "Tsat FRZ evap out calc." Due to experimental error they are offset. However, they closely follow each other and cause performance that indicates a two-phase condition. The status of the fresh food fan is shown on the following graphs by a line that is at 4 when the fan is on and 0 when it is off. The value of 4 has no significance beyond showing the fan is on.

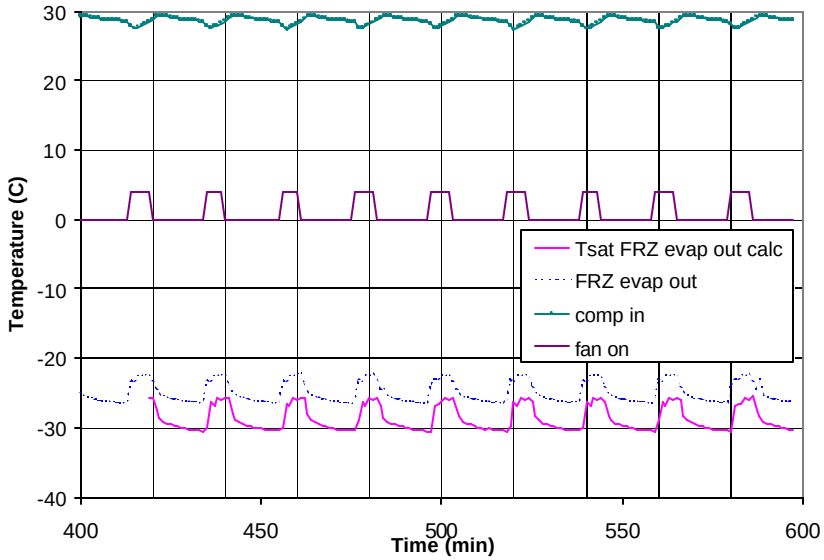

Figure 2.7.2.2 Freezer Evaporator Exit and Compressor Inlet Refrigerant Conditions (300g Charge 25°C Ambient Temperature)

At the 270 and 300 gram charges, the two-phase refrigerant leaving the freezer evaporator is superheated by the capillary tube suction line heat exchanger by 30-50 degrees (Figure 2.7.2.2). However, the increases in charge to 350 gram charge reduces the quality at the exit of the freezer evaporator. The liquid portion of the refrigerant can not be boiled off by the suction line heat exchanger. Therefore, during part of the cycle the refrigerant entering the compressor is two-phase (Figure 2.7.2.3 Similar graphs for other ambient temperatures are included in Appendix E). The exit of the condenser is two-phase during the last part of the fan-off time (Figure 2.7.2.3 Note: experimental error causes an offset in these graphs, too).

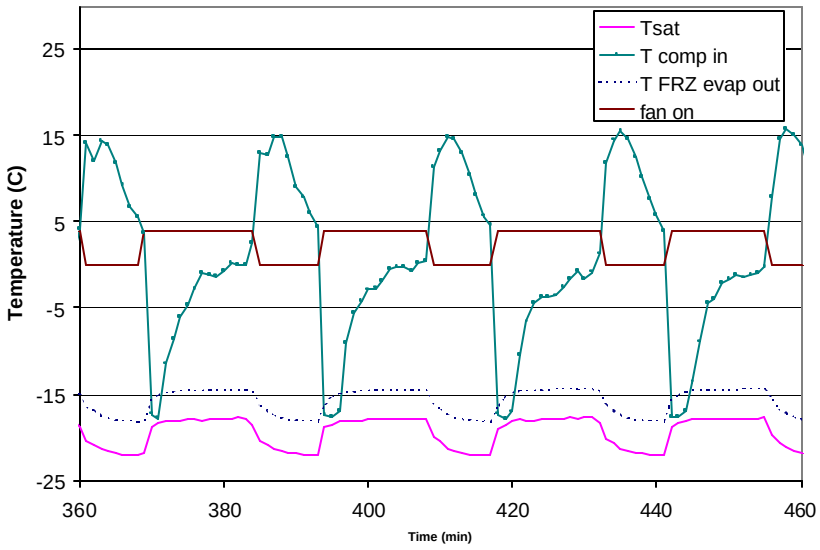

Figure 2.7.2.3 Freezer Evaporator Exit and Compressor Inlet Refrigerant Conditions (350g Charge 32°C Ambient Temperature)

When the fresh food fan turns on the saturation pressure and temperature in both evaporators increases. The temperature at the inlet to the compressor drops suddenly and becomes two-phase. This could be due to the refrigerant in the fresh food evaporator boiling and two-phase refrigerant bubbling up to the freezer evaporator exit. This would reduce the quality exiting the evaporator and increase the latent heat capacity of the exit stream. As the accumulated charge in the fresh food evaporator boils off, the quality at the freezer exit increases and the superheat into the compressor increases.

When the fresh food evaporator fan turns on, the pressure of the two-phase refrigerant at the compressor inlet also increases. Therefore, the compressor outlet pressure and condenser saturation pressure increase (Figure 2.7.2.4). Because the saturation temperature in the condenser increases, the heat transfer rate increases and the refrigerant reaches a quality of zero earlier in the condenser than during the fan-off time. The condenser has a larger subcooled wetted region, further increasing subcooling (Figure 2.7.2.4). Also, the refrigerant that was accumulated in the fresh food evaporator now accumulates in the condenser. When the fresh food fan turns off, the pressure throughout the system drops and the condenser subcooling decreases. The decrease in evaporator pressure and the retention of liquid in the fresh food evaporator causes an increase in the quality of the refrigerant leaving the freezer evaporator and a decrease in the flow rate in the suction line. Therefore, the heat capacity of the suction line flow decreases. Consequently, when the fan turns off, the refrigerant entering the compressor becomes more superheated. This is also partially due to the fact that the compressor subcooling decreases and the refrigerant in the capillary tube is warmer. However, the superheat increases faster than the condenser responds to the fan turning off. As the evaporators refill with two-phase refrigerant, the quality at the freezer exit decreases and the superheat at the compressor inlet decreases. The decrease in COP at 350 gram charge is most likely due to this charge shifting and the cold, at times two-phase, compressor inlet.

During the long fan cycle tests, this charge shifting propagates throughout the system. The time required for the refrigerant to make a complete circuit is approximately 8.5 minutes (refrigerant charge divided by mass flow rate). Because the fan cycle times were longer than this, the effect of the fan turning off and on was communicated to the other parts of the system. This effect could be shown by the double bumps in Figure 2.7.2.5 that appear in the fan-on part of the cycle. These bumps occur in all the long fan cycle tests. However, they occur at about half the time required for the refrigerant to make a complete circuit. In addition, the effect of the fresh food fan cycling on pressure through out the system propagates faster than the refrigerant flows.

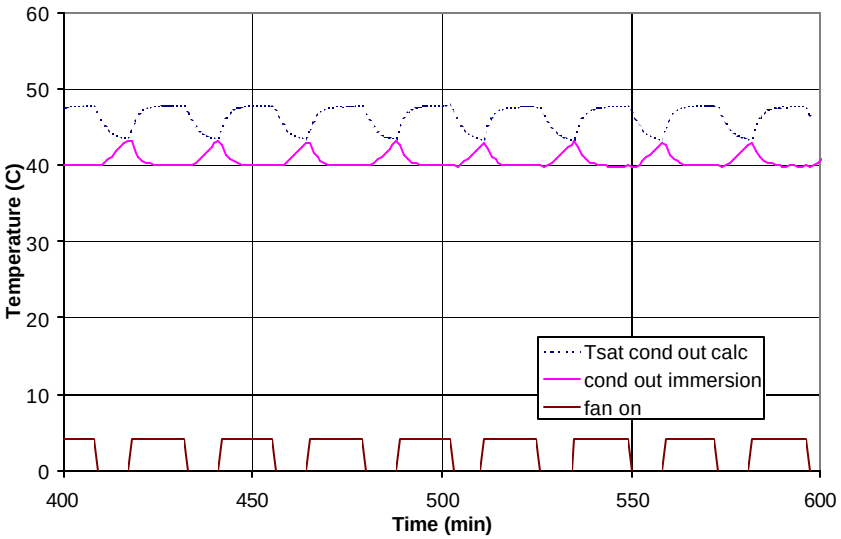

Figure 2.7.2.4 Condenser Exit Refrigerant Conditions(350g Charge 32°C Ambient Temperature)

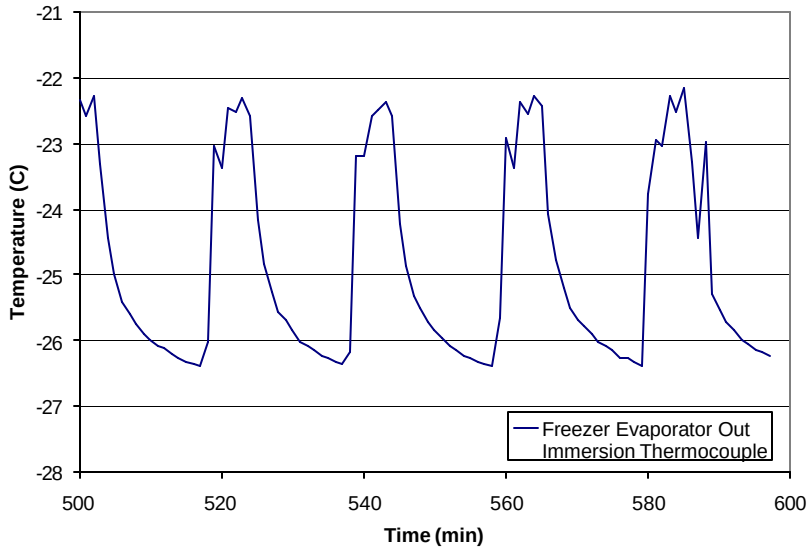

Figure 2.7.2.5 Propagation of Fresh Food Fan Influence throughout Refrigerant Circuit

Part of the rationale for running the shorter fan cycle tests was to run the system at a steadier condition. However, the data was not logged fast enough to resolve whether the refrigerant shifts. It is assumed that charge shifting occurs, but is smaller than that in the long tests. During the short fan cycle tests the inlet to the compressor is superheated but is still cold. It varies between –17.4°C for the 16°C ambient temperature and 8.1°C for the 32°C test.

The cold compressor inlet caused the COP to be lower for the short cycle tests than for the long cycle tests at the same charge (see Figure 2.7.1.2). Possibly, the optimal charge is different for the short cycle because the refrigerant is not shifting locations as much within the refrigerator. Also, the compressor operates differently during the short cycle tests (See Section 3.5.1 for a more detailed description of the compressor's behavior). The compressor operates with a lower measured flow rate during the short cycle tests for a given set of evaporating and condensing pressures (see Figure 3.5.1.3).

2.8 Conclusion

A dual evaporator refrigerator's performance was tested. The heat transfer through the cabinet was measured and the optimal refrigerant charge determined. The fresh food temperature was controlled by turning the evaporator fan off and on at two different cycle lengths. Since the refrigerator compressor was underpowered, the freezer temperature changed with the ambient temperature. This affected all aspects of the refrigerator's performance. In addition, the refrigerator normally had a two phase freezer evaporator exit. Reducing charge may improve performance by ensuring that the freezer evaporator exit and the inlet to the compressor are always superheated.

Chapter 3: Dual Evaporator Refrigerator Modeling

3.1 Introduction

Dual evaporator refrigerators were modeled using a computer simulation. Modifications were made to the previously developed code in order to simulate better the refrigerators in this study. Several of the input parameters were adjusted so that the model results better matched experimental results.

The model was initially developed for the study of single evaporator refrigerator-freezers at the Air Conditioning and Refrigeration Center (ACRC) at the University of Illinois at Urbana-Champaign. It consists of a general Newton-Raphson solver linked to a series of equations and functions that describe the particular refrigeration system being modeled (Mullen (1994) and Woodall (1996)). The simulation model for refrigerators is called RFSIM. The model assumes a steady state operation. The single evaporator model is described in more detail in Woodall and Bullard (1996). RFSIM was modified (Stein (1999)) for dual evaporator refrigerators by adding a second evaporator in the fresh food section and eliminating air exchange between the compartments. The fresh food evaporator is modeled as a two-phase region and the freezer evaporator includes both a two-phase region and a single-phase superheated region. Additional modifications were needed to accurately represent the prototypes tested.

The nomenclature used in Stein (1999) and continued here is that the freezer compartment variables are written simply such as "tevap." The fresh food variables have an "f" added, e.g. tevapf. Alternatively, a freezer variable is denoted with a "z" added, e.g. tevapz (See Appendix C for a complete listing of model variables).

3.2 Fresh Food Fan Output Scaling

The dual evaporator model was written so that whenever the compressor was operating, the evaporator fans were assumed to run continuously. In the actual performance tests, the fresh food fan was switched off and on to control temperature. To model this effect, a fan scaling factor was added to the fresh food compartment fan. This factor, beta_evapffan , represents the fraction of time the fan is on. The power consumed by the fan while running continuously (pevapffan) is multiplied by this factor to determine the power consumed while cycling on and off (pevapffan_calc):

pevapffan_calc = pevapffan*(beta_evapffan)

Similarly the total air flow rate through the fan is scaled linearly by the fan on time fraction:

vdotevapf_calc = vdotevapf*beta_evapffan

These equations were inserted as equations in the main body of the model. This allows beta_evapffan to be solved for as a variable. In earlier work (Woodall (1996) and Cavallaro (1995)) the fan scaling factor had been placed in an auxiliary file and could not be solved for directly. In this study the air-side heat transfer coefficient (hairevapf) was always input to the model as a known parameter. However, if hairevapf is to be solved for as a variable the unscaled air flow rate is used to compute it. The value of hairevapf is determined during the on time by the flow rate vdotevapf, and then the heat transfer is scaled by the fan on time fraction, beta_evapffan.

Note that the on-off cycling leads to the linear relationship. Varying flow rate by changing the rotational speed of the fan leads to a different relationship since the fan power consumption and flow rate are proportional to the fan speed to the third power. From prior work (Woodall (1996)), the RFSIM code includes the ability to scale the output of the freezer fan by this method. The ratio of the fan speed at partial power to the speed at full power is represented as beta_evapfan. The power and flow rate relationships are of the form:

pcondfan_calc = pcondfan*(beta_condfan**3.0d0)

pevapfan_calc = pevapfan*(beta_evapfan**3.0d0)

3.3 Hot Loop Circuit Modifications

The first version of the dual evaporator equations had a liquid line after the compressor. It was modeled as being in thermal contact with the refrigerator and freezer compartments. However, all of the heat transferred from the liquid line entered the freezer cabinet. This is a fairly accurate model for a system that has the liquid line on the mullion only because the mullion has very little surface in contact with the surrounding air. However, the refrigerators as tested used the compressor discharge line to warm the front flange around the complete perimeter of the freezer and fresh food cabinets. The original model added a large load to the freezer compartment, causing extremely high condenser temperatures.

To remedy these problems, a discharge line hot loop was added to the system. The discharge line is a single-phase vapor region in thermal contact with the air on the outside of the refrigerator. Boughton (1992 and 1996) discusses in more detail the heat transfer characteristics of the flange surrounding the door. The hot loop was initially in thermal contact with the both compartments. Consequently, the model was revised so that the hot loop was split into two sections: one for the fresh food and one for the freezer. The relative lengths of the sections are defined by the variable flnghtratio, the ratio of loop length in contact with the fresh food cabinet to the total length. The temperature and enthalpy for the inlet to the hot loop are t0 and h0 and for the exit they are t1 and h1. To keep the sequential numbering through the flow loop, the temperature and enthalpy between the compartments are designated as t0a and h0a. Although splitting the hot loop is not necessary when it is in contact with the surroundings, these formulas were retained for flexibility if a future refrigerator has the loop in contact with the cabinet.

The heat transfers from the hot loop sections are calculated using the log mean temperature (LMTD) technique:

LMTD_dischargef = ((t0-tamb)-(t0a-tamb))/log((t0-tamb)/(t0a-tamb))

0 = UAdischarge * flnghtratio * LMTD_dischargef - qdischargef

The UA value is input by the user. However, the heat transfer is relatively small with respect to the rest of the system. In addition, it is assumed that if the length of the discharge line is less than three feet, then it is not acting as a hot loop. Consequently, it is modeled as adiabatic.

Splitting the hot loop creates one more LMTD equation and two more variables, t0a and a second heat transfer value where there had been only one. Therefore, more equations are needed to close the system. An energy balance across the freezer section was used. The equation is as follows where w is the refrigerant mass flow rate:

0 = h0a - h1 - (qdischargez)/w

However, this creates a new variable h0a. The temperature and enthalpy at point "a" are then related using the RFSIM refrigerant property functions. A weighted average of the input and output pressures and the enthalpy at point "a" are input into the function TPHiter. A temporary value for the temperature at point "a" (t3atemp) is returned and set equal to the actual temperature at "a":

call TPHiter(p3*flnghtratio+(1-flnghtratio)*p4,h3a,t3atemp)

0= t3a-t3atemp

The original pressure drop formula is used for the discharge line. It only requires the refrigerant quality and specific volume at the inlet and exit of the line. Therefore splitting it does not affect the pressure drop calculation.

The complete versions of the code blocks added to the model are included in Appendix D.

3.4 Model Operation Modes

In theory, the user can select any combination of variables (unknowns) and parameters (knowns) as long as the number of variables matches the number of equations. In reality, there are certain sets of variables and parameters that are more flexible and convenient to work with than other sets. These sets are termed modes and can have a correspondence to the controlled and uncontrolled variables in real tests.

In this study, three modes were used: lab, kitchen, and fitting modes. Lab mode corresponds to the testing methods commonly used for performance tests. These tests use heaters in the cabinet compartments to ensure that the refrigerator runs continuously at steady temperatures. Therefore, in this mode of operation the user inputs runtime (equal to 1), the cabinet temperatures, and beta_evapffan. The model then calculates the heat addition to the freezer and fresh food compartments by the heaters. Kitchen mode corresponds to the operation of the refrigerator in the household kitchen of a consumer. In this mode, the cabinet temperatures and compartment heater values (equal to zero) are designated by the user. The model then solves for runtime and beta_evapffan. Fitting mode corresponds to the way that the experiments were run in this study and was used to adjust the model to the experimental data. In the fitting mode, beta_evapffan, the heater values (equal to zero), and one compartment temperature were supplied by the user and runtime and the other compartment temperature were calculated by the model. In all three modes the evaporator superheat and condenser subcooling were input by the user and the refrigerant charge was calculated by RFSIM. Because capillary tube was not explicitly modeled, its effectiveness was specified. A complete listing of the variables and combinations used in the various modes is included in Appendix C.

3.5 Fitting the Model to the Experimental Data

Several modifications were made to the model parameters to make the simulation results match the experimental results. However, no attempt was made to match the model and experiment better than a 20% discrepancy because uncertainty in the compressor maps and heat transfer values made it difficult to exactly match the experimental results. The following changes illustrate the type of adjustments that could be used to make the simulation results match the experimental conditions.

3.5.1 Compressor Map Anomalies

The compressor installed in the prototype refrigerator had been individually characterized in off-campus calorimeter tests. The effect of the condensation and evaporation temperatures on power consumed and mass flow rates was measured. These were then curve fit to a polynomial of the form:

$$f=(c_1+c_2*Te+c_3*Te^2)+(c_4+c_5*Te+c_6*Te^2)*Tc+(c_7+c_8*Te+c_9*Te^2)*Tc^2+c_{10}*Te^3+c_{11}*Tc^3$$

The c's are the curve fit coefficients, Te is the evaporation temperature, Tc is the condensation temperature, and f is either the flow or power. These polynomials are termed the power map and the flow map.

However, the compressor did not perform in situ as predicted by the performance maps. The actual power consumed by the compressor was less than that predicted by the polynomial by a constant offset (see Figure 3.5.1.1). This value depended on the test, but was in the range of 20-30 watts or approximately 20%. Simply subtracting the time average of the measured power from the time average of the predicted power yielded the offset. When this offset was subtracted from the predicted power, the new value closely followed the actual measured power.

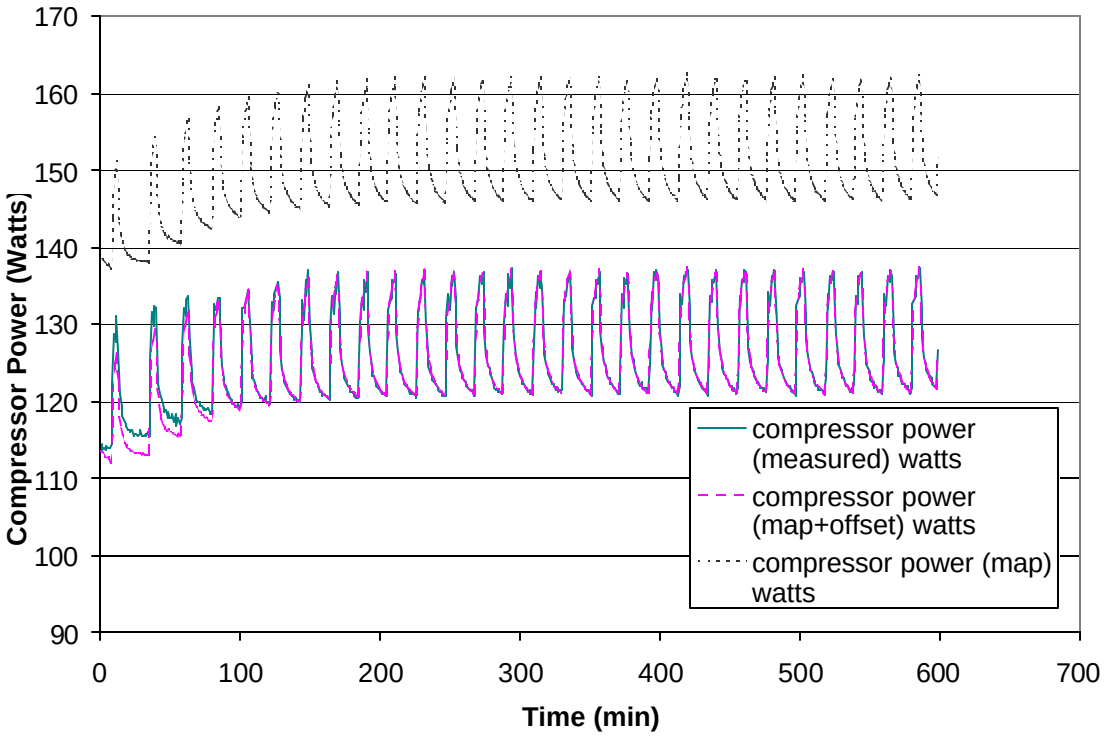

Figure 3.5.1.1 Compressor Power Map Offset Error (300g Charge 25°C Ambient Long Fan Cycle Test)

The watt transducer used in the tests was checked, recalibrated and found to be operating correctly. When the refrigerator was connected to a different watt transducer the same type of offset was observed. In addition, the power map from the calorimeter tests closely matched the map supplied by the manufacturer.

The flow map was verified by calculating an energy balance over the cabinet. The enthalpy at the inlet to the capillary tube (h4) was calculated from the measured temperature and pressure, as was the suction line exit enthalpy (h11). The heat addition to the cabinet from the surroundings was calculated using the cabinet and ambient

temperatures (tafrig, tafrez, and tamb) and the cabinet UA values (UAf and UAz). The heat addition from the evaporator fans (pevapfan_calc and pevapffan_calc) were measured. The following energy balance was computed:

$$0=h11-w*[UAf*(tamb-tafrig)+UAz*(tamb-tafrez)+pevapfan\_calc+pevapffan\_calc]-h4$$

The only unknown in this formula is the mass flow rate (w). The flow rate was computed for a number of tests with a 300g charge and at all three ambient temperatures and with both long and short fan cycles. The flow calculated from the energy balance is significantly lower than that predicted from the flow map (see Figure 3.5.1.2).

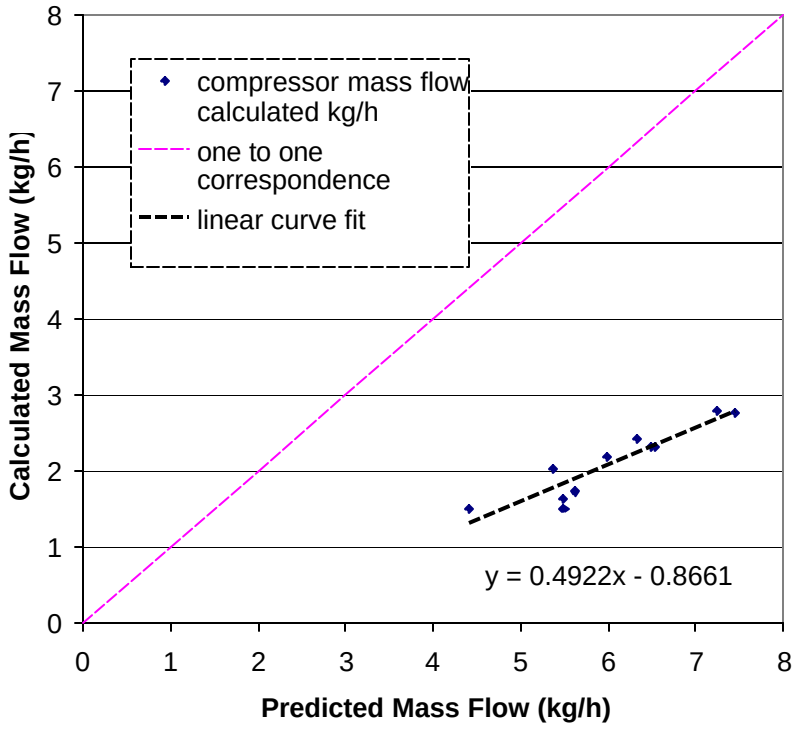

Figure 3.5.1.2 Compressor Mass Flow Calculated from Cabinet Energy Balance as a Function of Mass Flow Rate Predicted from Compressor Map

The calculated mass flow was curve fit to a function of the predicted mass flow rate. This curve fit equation was used to adjust the flow rate prediction in the model. However, the selection of tests at the long fan cycle condition or at the short fan cycle condition affects this equation (see Figure 3.5.1.3). This indicates that the compressor map error is affected by the type of cycling. In addition, the calculation using the energy balance includes the uncertainty in the heat leak values and the measurement of the temperatures and pressures used. Although the accuracy of the flow map adjustment is questionable, its use greatly improves the match of the simulation results to the experimental results.

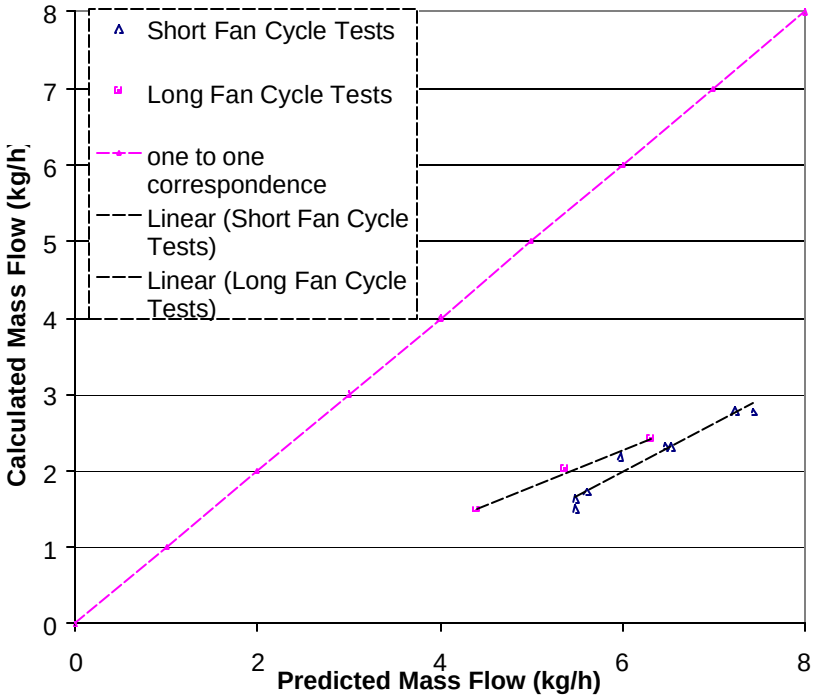

Figure 3.5.1.3 Change in Compressor Map Discrepancy between Long and Short Fan Cycle Tests

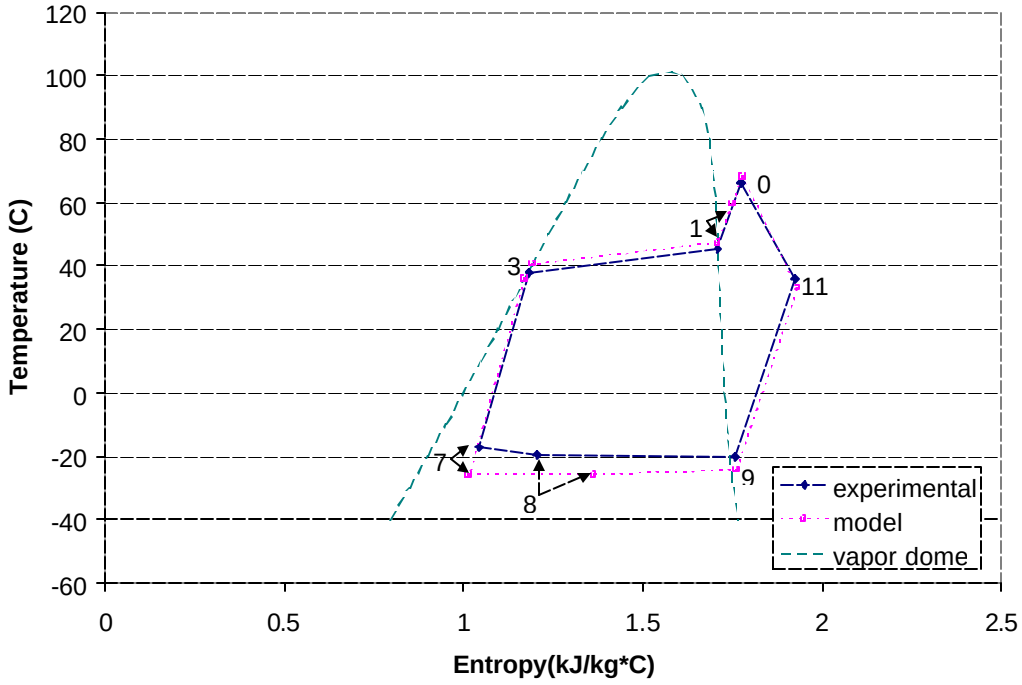

Figure 3.5.1.4 Entropy-Temperature Diagram from Original Compressor Maps(Numbers Correspond to Locations as Described in Appendix C)(32C Ambient Long Fan Cycle)

The temperature-enthalpy (T-s) diagram of the simulation results using the original compressor maps is shown in Figure 3.5.1.4. The high side temperatures are higher than the experimental values and the low side temperatures are too low. This indicates that the compressor in the actual refrigerator is not performing as well as the model predicts. When the compressor power is reduced by 20 watts there is only a minor effect on the T-s diagram (Figure 3.5.1.5). The compressor exit temperature decreases slightly. But as discussed below in the section on the compressor heat transfer, the temperature at the compressor exit is determined by another "fitted" value. However, the energy consumption predictions closer match the measured values.

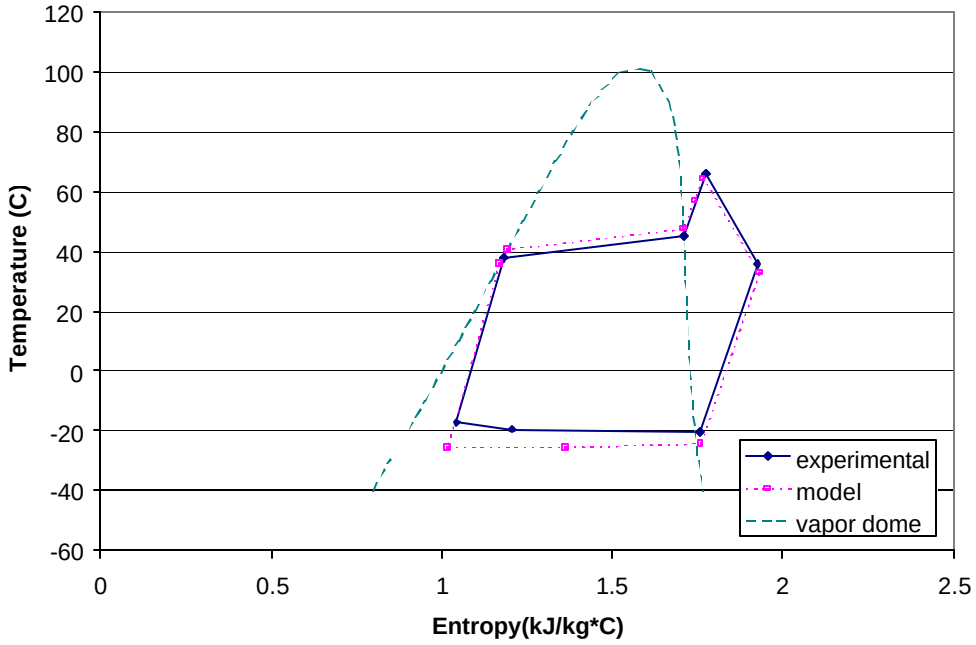

Figure 3.5.1.5 Entropy-Temperature Diagram with Power Offset Only(32C Ambient Long Fan Cycle)

When the flow map is adjusted, the T-s diagram much closer agrees with the experiments (Figure 3.5.1.6). Both the low side and the high side, temperatures are in better agreement. However, the model under predicts the COP and over predicts the compressor power.

When both the power offset and the flow map adjustment are used the model results most closely match the measured values. Not only do the T-s diagrams match (Figure 3.5.1.7) but the COP and compressor power match within 15%. However, the refrigerant charge prediction is too small by 60%. This aspect of the model has been in error during prior work due to insufficient void fraction correlations and data. In addition, the shifting of charge in the refrigerator and build up of charge in the fresh food evaporator may cause the test refrigerator to have a higher charge than the steady state simulation predicts. Also, adjustment in the condenser tube size as discussed below added to this error. A pressure-enthalpy (P-h) diagram with both power and flow maps adjusted is shown in Figure 3.5.1.8.

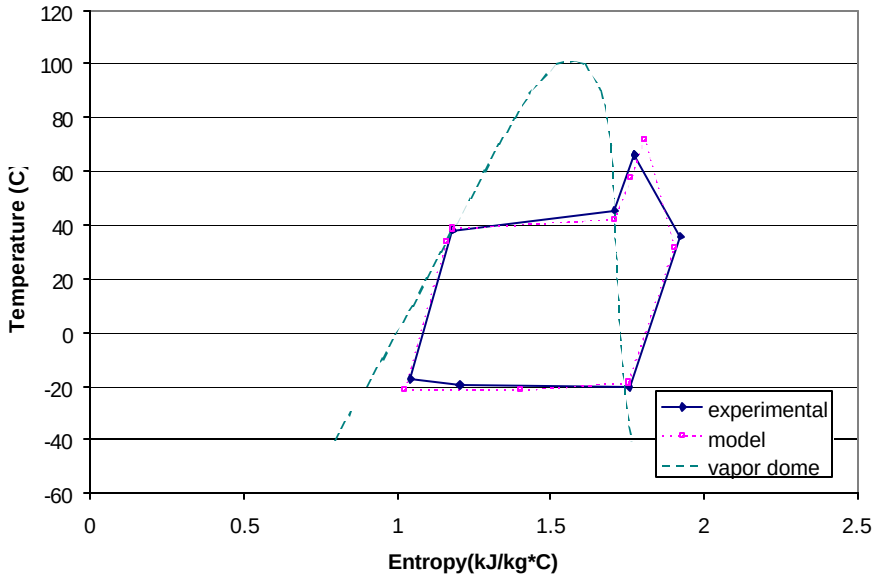

Figure 3.5.1.6 Entropy-Temperature Diagram with Flow Adjustment Only(32C Ambient Long Fan Cycle)

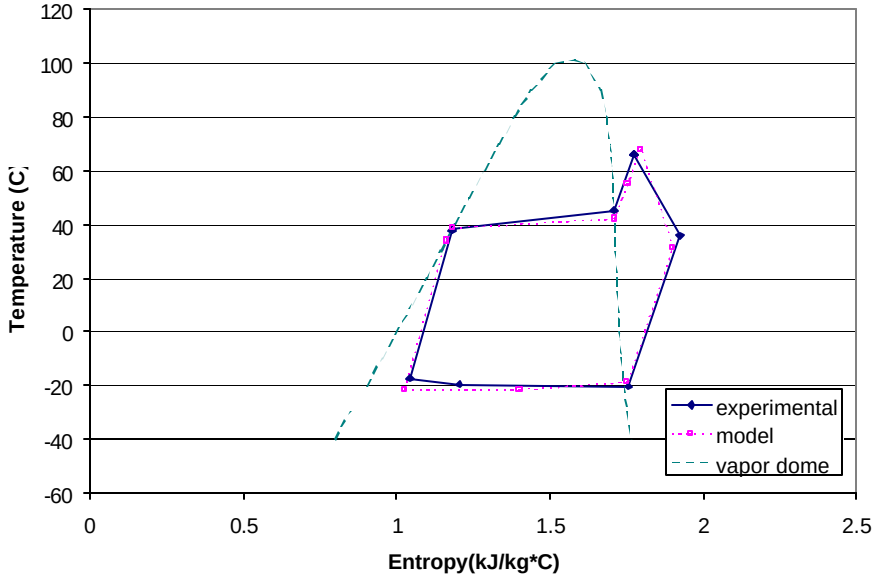

Figure 3.5.1.7 Entropy-Temperature Diagram with Flow and Power Maps Adjusted (32C Ambient Long Fan Cycle)

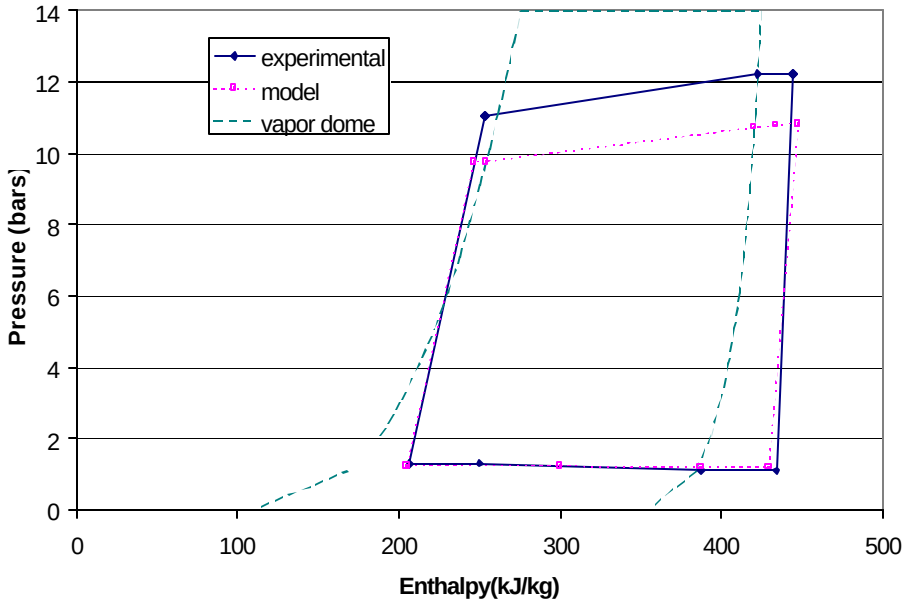

Figure 3.5.1.8 Pressure-Enthalpy Diagram with Flow and Power Maps Adjusted (32C Ambient Long Fan Cycle)

3.5.2 Capillary Tube-Suction Line Heat Exchanger Effectiveness

RFSIM uses an effectiveness-NTU technique to model the capillary tube-suction line heat exchanger (CTSLHX) as a counterflow heat exchanger. The CTSLHX effectiveness (ectslhx) for the simu lations was calculated by the following formula:

ectslhx=(t7-t4)/(t9-t4)

In this formula t4 is the temperature at the filter dryer outlet, t9 is at the freezer evaporator outlet, and t7 is the fresh food evaporator inlet. This assumes that the heat capacities of both streams are equal. This is not accurate for several reasons. First, the refrigerant in the cap tube is two phase or liquid but in the suction line it is vapor. As a result, the flows have different specific heats (infinite specific heat in the two phase region). Second, the refrigerant charge may be shifting into and out of the fresh food evaporator. Consequently, the flow rate in the suction line and the capillary tube may be different from each other over the course of the fan cycle (see Liu (1997) for a more detailed analysis of capillary tube behavior).

The CTSLHX effectiveness value used for all the simulations was calculated from the average experimental values from the test at 300g charge, 32°C ambient temperature, and the long fan cycles. This value was 0.948. The values calculated from the other tests differed from this value by less than 3%.

3.5.3 Compressor Shell Heat Transfer

The compressor shell heat transfer was computed similar to that described in Cavallaro (1995). RFSIM calculates the shell temperature (ts) as a linear function of the compressor discharge temperature. The slope and

intercept of this linear equation are determined by the particular compressor used. The model also requires an air side overall heat transfer coefficient (hAcomp) that is determined by the compressor and the airflow over it.

For the refrigerator tested, these values were calculated with test data from a number of tests at the short and long fan cycle. Thermocouples on the top and front of the compressor measured the shell temperature. The averages of these locations were correlated with the compressor outlet temperatures (see Figure 3.5.3.1).

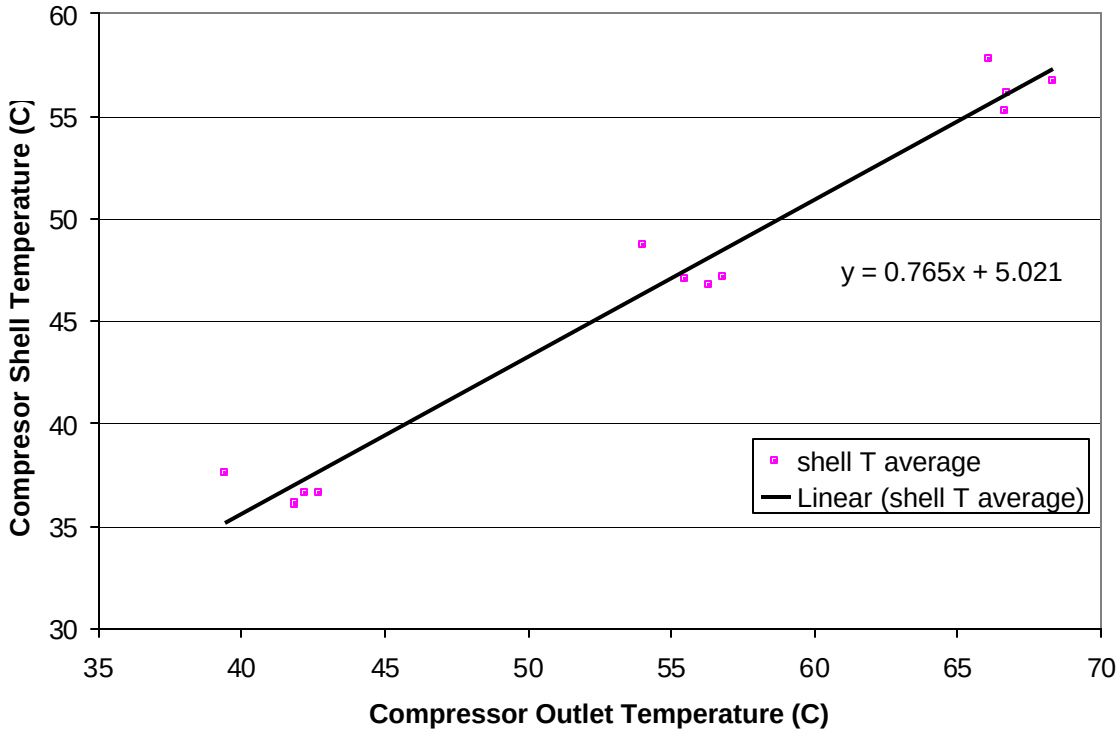

Figure 3.5.3.1 Compressor Shell Temperature to Outlet Correlation

The heat transfer from the shell was calculated by an energy balance over the compressor. The enthalpy in (h11) and out (h0) were calculated from the measured inlet and outlet temperatures and pressures because both the inlet and outlet are superheated vapor. The compressor power (pcomp) was measured. Therefore the heat transfer from the compressor shell is as follows:

hAcomp*(tacondfanout-ts)=w*(h0-h11)+pcomp

The compressor mass flow is designated as "w" in RFSIM. The shell heat transfer and the temperature difference between the shell and the air flow over it (tacondfanout) is used to calculate the heat transfer coefficient (hAcomp).

Because the mass flow is not known accurately, the compressor shell heat transfer is not accurate. The value for hAcomp calculated using the original compressor map is 5.59 Btu/hr°F. When this value is used in the simulation, it underestimates the heat transfer from the shell (see Figure 3.5.3.2). This is unexpected because a decrease in flow rate from the original map should decrease the calculated heat transfer and therefore decrease the heat transfer coefficient. By increasing hAcomp to 11 Btu/hr°F the compressor heat transfer better matches the experiments (see Figure 3.5.1.7). This discrepancy could be caused by the location of the thermocouples relative to

the airflow. If the thermocouples are in locations that are warmer than the shell temperature where most of the heat transfer occurs, then hAcomp is underestimated.

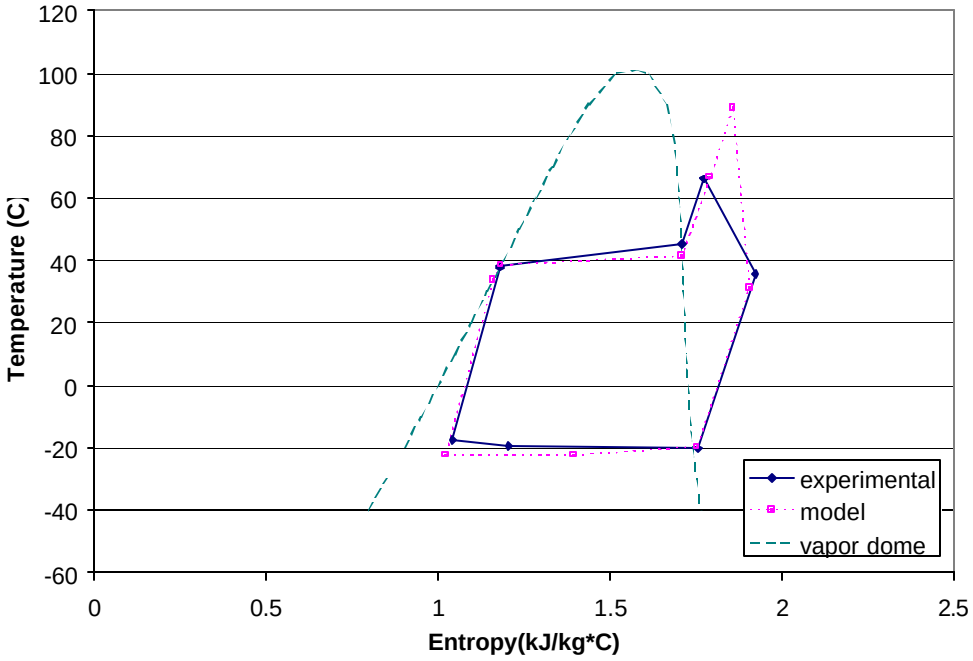

Figure 3.5.3.2 Entropy-Temperature Diagram with Calculated hAcomp (32C Ambient Long Fan Cycle)

3.5.4 Condenser Pressures

The measured high side pressures were higher than those initially predicted by the computer simulation(Figure 3.5.4.1). In addition, the measured pressure drop across the condenser was higher than that predicted. This difference in pressure drop could be due to the condenser being of a different geometry than those previously modeled. The condenser in the prototype refrigerator of this study is a compact heat exchanger type. It is practically a cube. In order to fit the model to the experimental data, the diameter of the condenser tubing was decreased until the pressure drop across the evaporator matched the measured value from the 32°C long fan cycle test. The diameter was decreased from 3.36 mm to 1.86 mm (see Figure 3.5.1.7 for simulation identical to Figure 3.5.4.1 but with decreased condenser tubing diameter). This value was then used for all the other simulations. Decreasing the tubing diameter decreases the internal volume of the condenser and decreases the charge prediction contributing to the error mentioned previously.

After the condenser pressure drop was matched, an offset between the predicted and measured high side pressures remained. However, the COP, runtime, and other significant system parameters were within 20% of the measured values, and no physical reason for the pressure offset was apparent. Consequently, no modifications were made to the model to account for it.

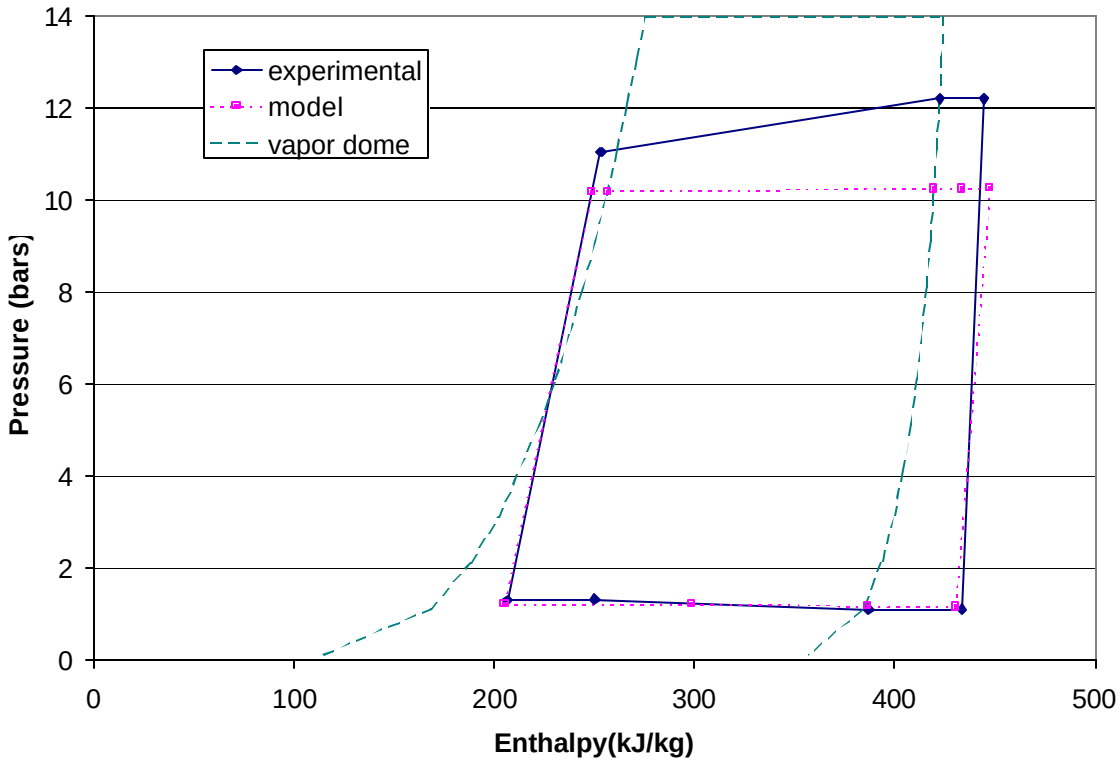

Figure 3.5.4.1 Pressure-Enthalpy Diagram with Actual Condenser Tubing Diameter (32C Ambient Long Fan Cycle)

3.5.5 Hot Loop UA

The hot loop UA value was set to a value of 0.32 W/°C. This controls the exit enthalpy of the hot loop and determines the position of point 1 on the T-S diagram. By increasing or decreasing the UA it can be moved either direction up or down the constant pressure line. This point is not significant as the hot loop transfers heat to the environment and simply acts as part of the condenser. When the condenser subcooling is specified in the model, the exit to the evaporator will be generally the same irrespective of the hot loop UA.

3.6 Conclusions

Although uncertainty still exists relative to the compressor functioning, the dual evaporator version of RFSIM models the prototype refrigerator to within 20%. Reducing the compressor flow rate and power consumption both improve the model's accuracy. Modifying the input values for the compressor heat transfer, the condenser pressure drop, and the hot loop heat transfer calculations brings the model into closer agreement with the experimental data. The model performs as expected and with a better description of the compressor and condenser, performance could presumably be made to closely match the experimental data.

Chapter 4: Refrigerator Design and Performance Prediction

4.1 Introduction

The refrigerator simulation model described in the previous chapter was used to predict the performance of the refrigerator with variations in the evaporator sizes. Design parameters were selected to simulate a production refrigerator. The RFSIM model was then used to simulate the performance of the refrigerator as used in a household kitchen and as commonly performance tested in the laboratory. The sizes of the fresh food and freezer evaporators were varied separately and the simulation results analyzed.

4.2 Simulation Parameters

The parameters used in the numerical tests were chosen to best simulate the performance of a production refrigerator. Therefore, the design values for the overall heat transfer coefficients were used rather than the prototypes' measured values. In addition, the original unmodified compressor maps were used. The measured curve for compressor shell temperature versus compressor outlet temperature was used. However, the compressor shell heat transfer coefficient value (hAcomp) that was determined by fitting the model to data was retained. The reduced condenser tube diameter was also retained to account for the pressure drop of the new condenser geometry. These two fitted values were retained with the intention of increasing the accuracy of the model.

The fresh food compartment was held at 4.44°C (40°F) and the freezer at –15°C (5°F). The evaporator superheat and the condenser subcooling were both held at 1.67°C (3°F).

The performance of the refrigerator was simulated with the fresh food evaporator at the actual size, half of the actual size, and twice the actual size of the prototype's freshfood evaporator. The external surface areas of the evaporators are 0.19 m^2, 0.39 m^2, and 0.78 m^2, respectively. The refrigerator was simulated at 16, 25, 32, and 43°C ambient conditions. Both "lab mode" and "kitchen mode" simulations were performed for all combinations of evaporator size and ambient temperature. In lab mode, beta_evapffan was set to 0.25 and runtime was set to 1 (continuous refrigerator operation). In kitchen mode, the heater values were both set to zero.

In order to investigate the effect of the freezer evaporator size on performance, refrigerator performance was simulated at four additional conditions. These were at 32°C with a freezer evaporator half and double the actual size. Both lab and kitchen mode were simulated.

4.3 Fresh Food Evaporator Variations

4.3.1 Kitchen Mode

As kitchen mode most closely represents the performance of a production refrigerator in everyday use, it is the most pertinent to the design process. However, the RFSIM model could not solve the equations for 25, 32, and 43°C ambient temperatures with the half-sized evaporator. The model would call certain thermophysical property functions out of the defined bounds and cause a program error. This normally occurs when a two-phase function is called in a single-phase zone. The failure to solve the equations in these cases probably indicates that the half-sized evaporator is too small to adequately cool the fresh food compartment at ambient temperatures of 25°C and above. Similar problems occurred when the model was solved with an evaporator 75% of the actual size. These results

indicate that the current evaporator may be at the bottom end of the acceptable range. At several other simulation points the model called other properties out of range. When this is done the model approximates a value in the superheated region by the value at a quality of 1. A subcooled quantity is approximated at a quality of 0. This affects the accuracy of the model. However, if the point is not far into the single-phase region this is not significant. The simulations that were affected by this error are as follows: all of the 16 and 25°C tests in kitchen mode, all of the half size tests in lab mode, and the 16 and 25°C tests at the actual size. In addition some of the runs called the compressor map outside of its range. However, when the map is graphed it appears linear throughout its range and beyond the prescribed endpoints. Therefore extrapolating beyond the measured points does not introduce a significant error.

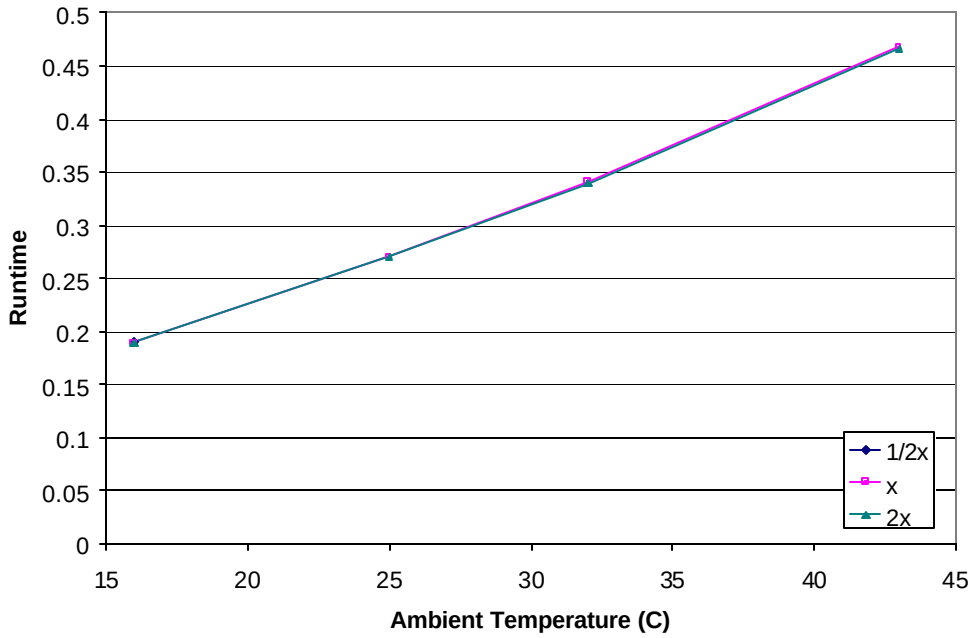

Figure 4.3.1.1 Variation in Runtime Fraction with Ambient Temperature

The load on the refrigerators is independent of the evaporator size because it is determined by the exterior and interior temperatures in kitchen mode. Consequently, the runtime fraction is determined by the ambient temperature and not the evaporator size (see Figure 4.3.1.1). In addition, the COP is a strong function of ambient temperature and not of evaporator size (see Figure 4.3.1.2). As a result, the yearly energy consumption is not affected by the evaporator size (Figure 4.3.1.3).

The fresh food fan on time is less for a larger evaporator since there is a greater surface area for heat transfer (Figure 4.3.1.4). This leads to small savings in fan energy and a decrease in noise with increasing evaporator size. The small increase in COP and small decrease in energy consumption with increasing evaporator size is due to this effect. In addition, the larger the evaporator, the more refrigerant is required to fill it (Figure 4.3.1.5). The difference between the amount of refrigerant needed at the lowest temperature and the highest

temperature increases with evaporator size. Therefore, the larger the evaporator, the more sensitive the freezer outlet condition is to ambient temperature given a specific charge.

A larger evaporator does not greatly improve energy efficiency, increases manufacturing cost, and decreases compartment volume. Therefore for steady operation, the fresh food evaporator should be made as small as possible as long as it can still adequately cool the fresh food compartment at all expected ambient temperatures.

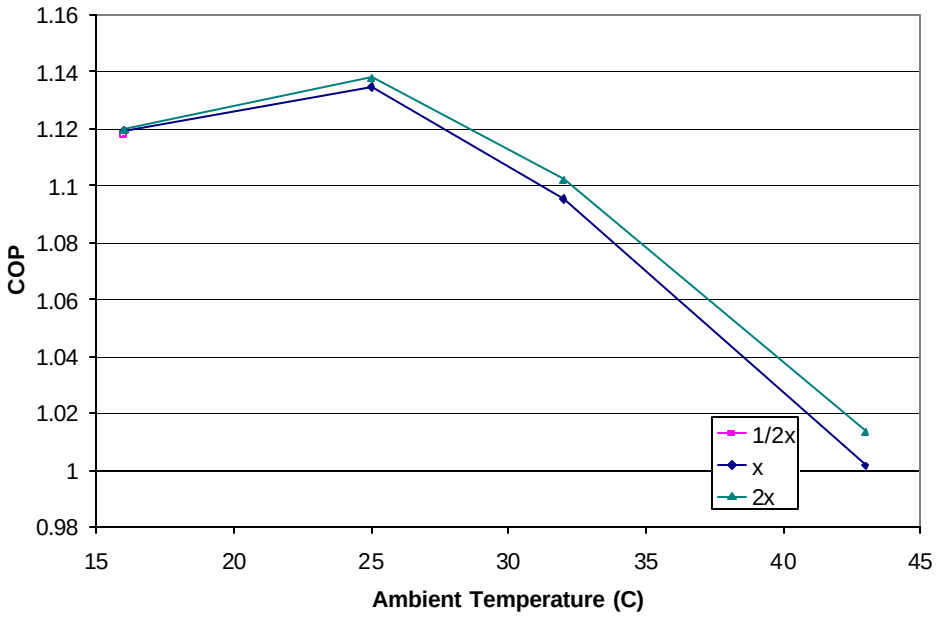

Figure 4.3.1.2 COP as a Function of Ambient Temperature

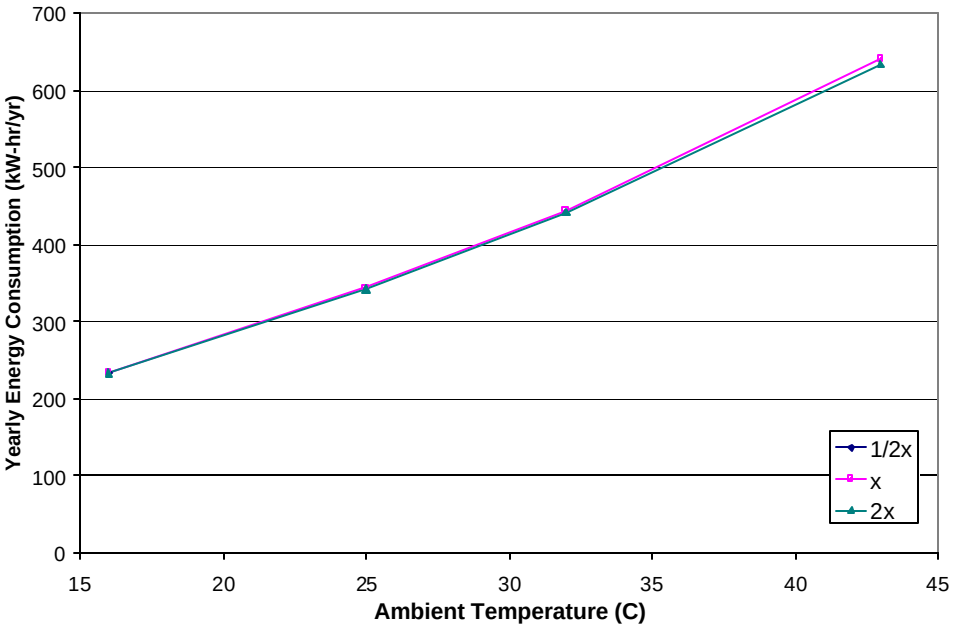

Figure 4.3.1.3 Yearly Energy Consumption versus Ambient Temperature

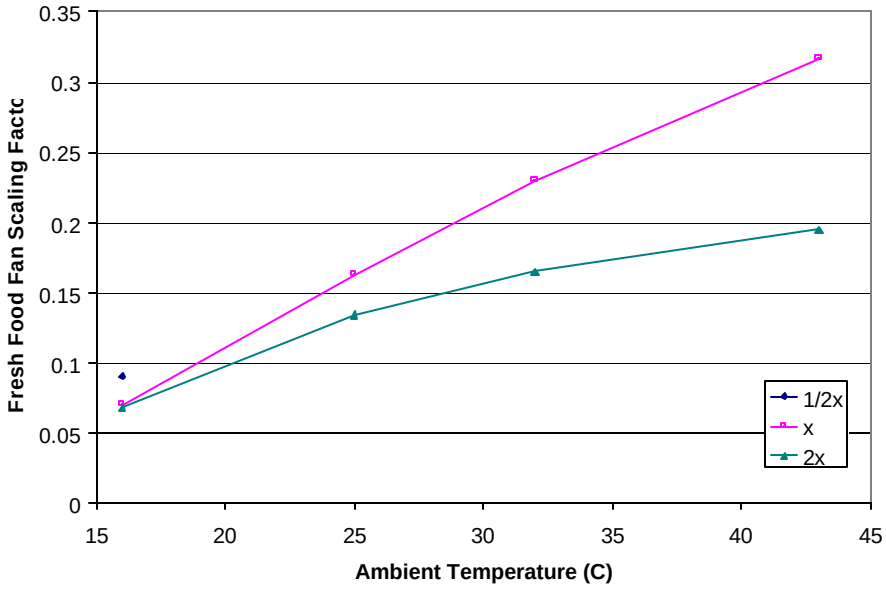

Figure 4.3.1.4 Fresh Food Fan On Time

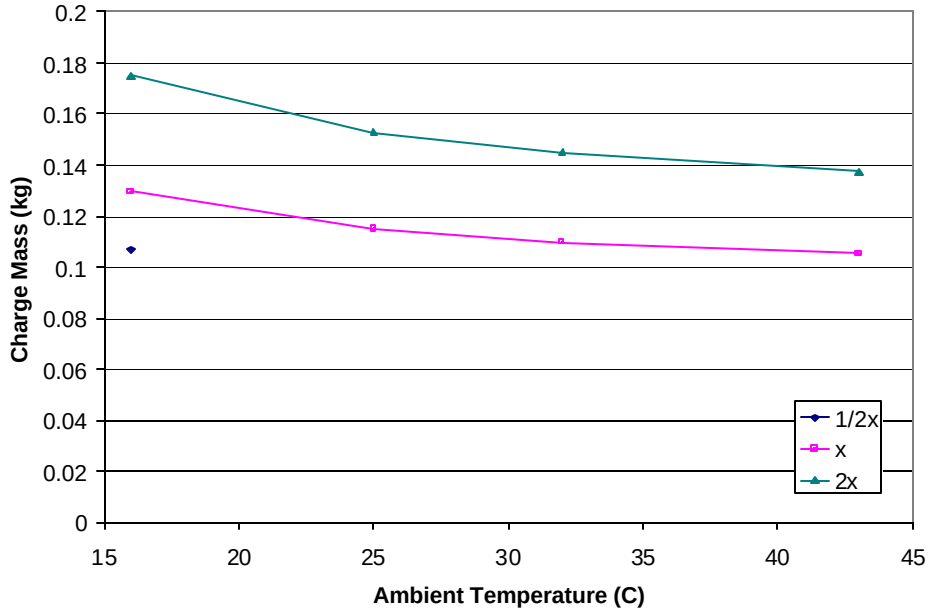

Figure 4.3.1.5 Variation In Required Charge with Temperature

4.3.2 Lab Mode

All conditions could be solved for in the lab mode due to the added flexibility from the heaters varying the load. In this mode, cooling capacity (the sum of the fresh food and freezer heaters) increases with evaporator size (Figure 4.3.2.1). COP also increases with evaporator size (Figure 4.3.2.2). The charge needed and the difference in charge at highest and lowest temperatures also increase with evaporator size (Figure 4.3.2.3).

These results indicate that when a load is added to the refrigerator such as warm food, a larger fresh food evaporator is superior. Therefore, a larger fresh food evaporator would improve efficiency during pull down but not during steady operation.

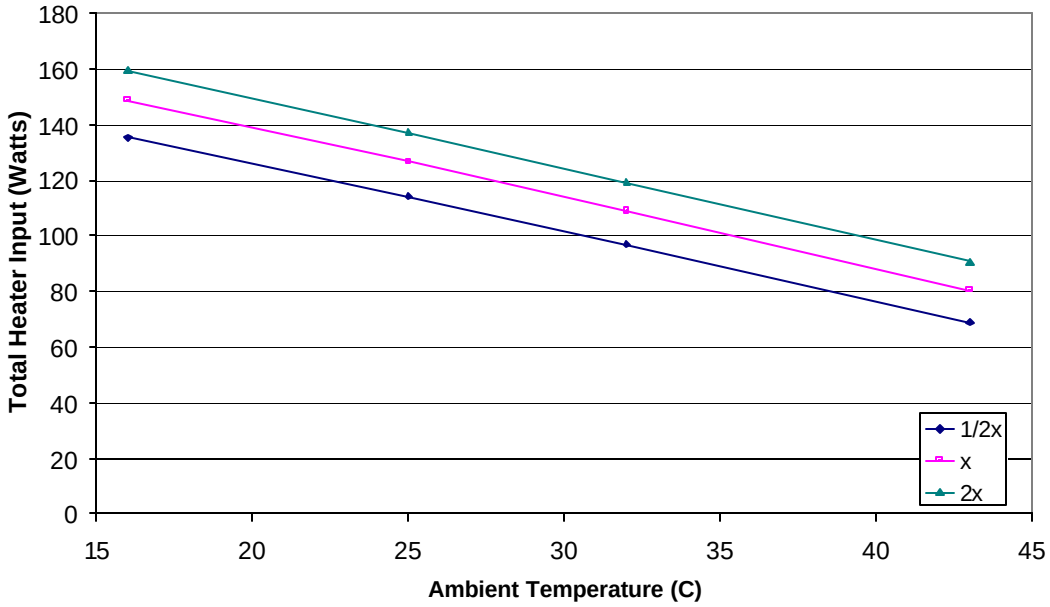

Figure 4.3.2.1 Total Cooling Capacity Variation with Ambient Temperature

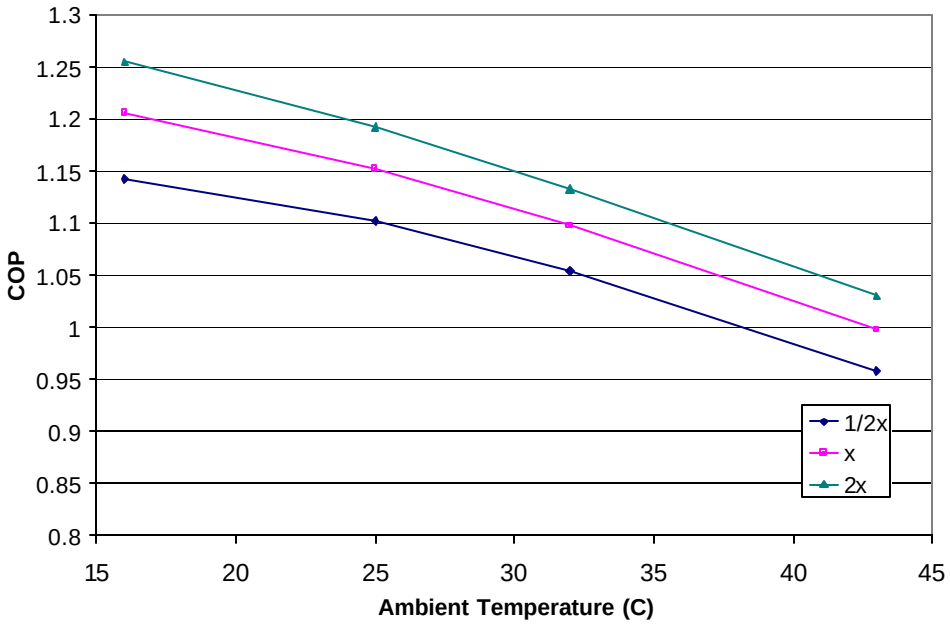

Figure 4.3.2.2 COP Increase with Evaporator Size Increase

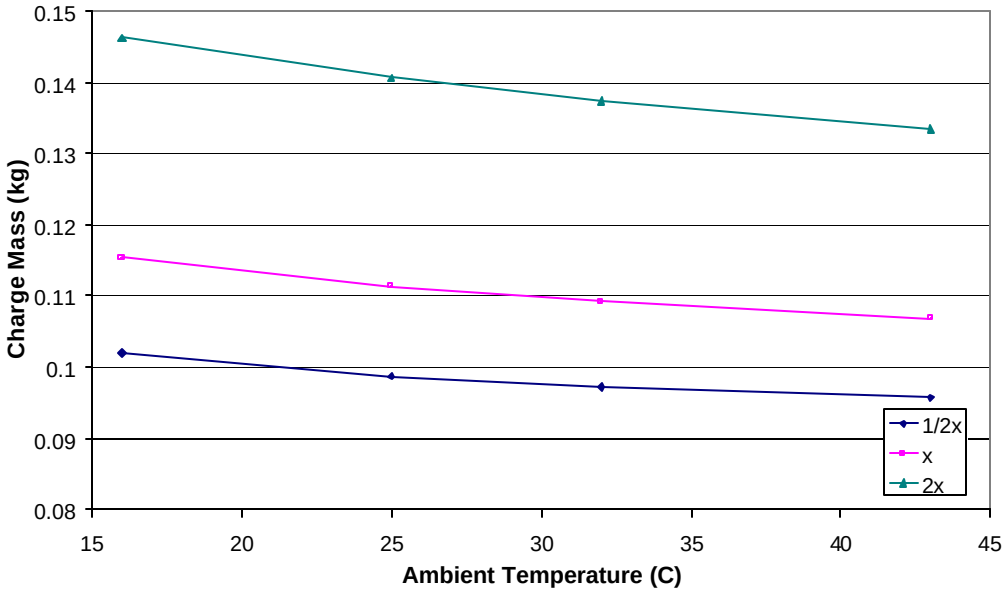

Figure 4.3.2.3 Charge Requirement Increase with Evaporator Size Increase

4.4 Freezer Evaporator Variations

All freezer evaporator simulations were performed at a 32°C. The fresh food evaporator size was held constant at the actual design value.

In kitchen mode, an increase in freezer evaporator area increases the COP (Figure 4.4.1) and the refrigerant charge required (Figure 4.4.2). This COP increase is not due to a change in fan power and could imply that an increase in freezer evaporator is more beneficial than an increase in fresh food evaporator size.

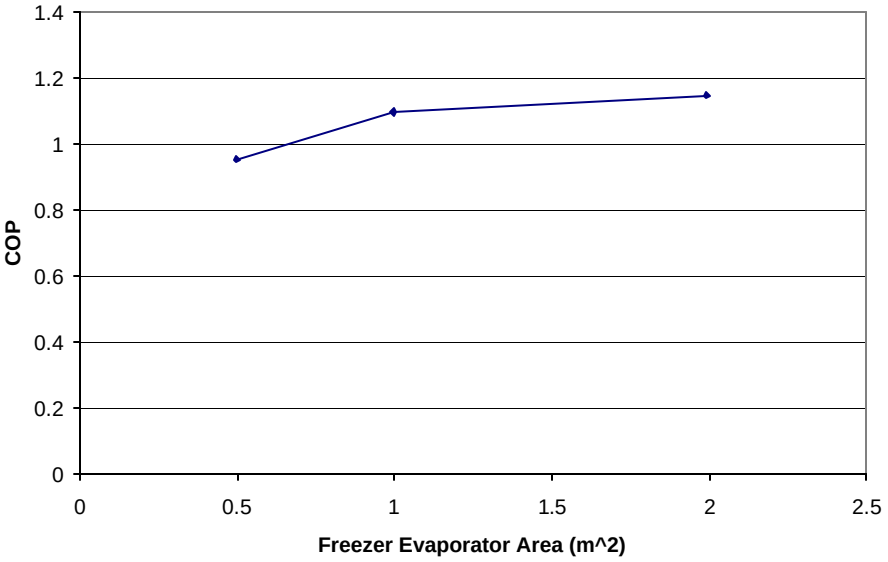

Figure 4.4.1 Increase in COP with Increase in Freezer Evaporator Size

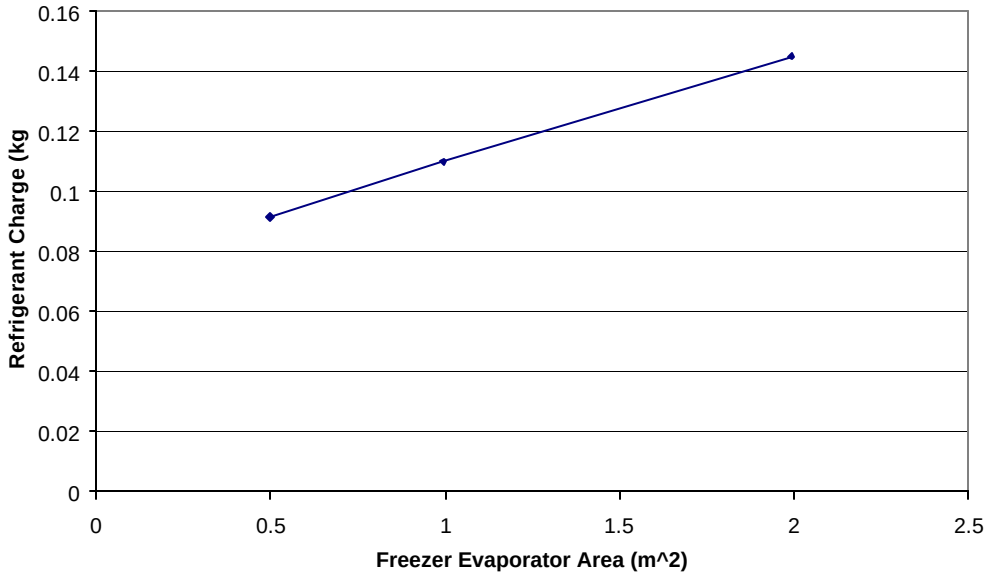

Figure 4.4.2 Increase in Refrigerant Charge with Increase of Freezer Evaporator Size

The model was run in lab mode with the same variations in freezer evaporator size. With the half-size evaporator, the freezer heater value was calculated as –3.3 watts. This indicates that the refrigerator can not adequately cool the freezer with a half-size evaporator.

4.5 Conclusions

The effect of changing the evaporator sizes on refrigerator performance was studied. The sizes of both the fresh food and freezer evaporators were changed and simulated in kitchen and lab mode. The fresh food evaporator was studied in more detail. an increase in size does not significantly improve COP but does increase capacity, However, an increase in the freezer evaporator size improves COP.

Chapter 5: Summary

The performance of dual evaporator household refrigerators was studied experimentally and by numerical simulation.

The prototype tested performed worse than expected due to insufficient compressor power and a higher cabinet thermal conductance. However, control of the fresh food cabinet air temperature was achieved through turning the fan off and on during operation. This fan cycling affected both the performance of the prototype and the charge distribution inside the system.

The data from the tests was used to check the accuracy of a numerical model of dual evaporator refrigerators. It was shown that the accuracy of the model could be improved through various adjustments. However, uncertainty about the compressor performance limited the accuracy to between 10 and 20 percent.

This model was then used to simulate the performance of the refrigerator as originally designed and with larger and smaller evaporators. In general, charge requirements increased with evaporator size, as did the system's sensitivity to ambient temperature. Increasing the fresh food evaporator size did not significantly increase COP but did increase capacity.

Bibliography

Bare, Jane. "EPA's Research Projects Relating to the Dual-Circuit and Lorenz Refrigerator/Freezers," Journal of the Air and Waste Management Association, Vol. 42, No. 1, 68-69, Jan. 1992a.

Bare, Jane. "Simulation Results of Single Refrigerants for Use in a Dual-circuit Refrigerator/Freezer," Journal of the Air and Waste Management Association, Vol. 42, No. 2, Feb. 1992a.

Bohman, R. H. and R. L. Harrison. "The Engineering and Manufacture of a High Efficiency, Automatic Defrost Refrigerator-Freezer," ASHRAE Transactions, Vol. 88, Part 2, 1053-1063, 1982.

Boughton, Brian E., Arthur M. Clausing, and Ty A. Newell. "Investigation of Household Refrigerator Cabinet Thermal Loads." Hvac&R Research. Vol. 2, No 2, 135-148, Apr 1996.

Boughton, B. E., A. M. Clausing, and T. A. Newell. "An Investigation of Household Refrigerator Cabinet Loads." Air Conditioning and Refrigeration Center Technical Report-21. University of Illinois at Urbana-Champaign, 1992.

Bullard, Clark. Personal communication. April, 2000.

Cavallaro, Alberto R. and Clark W. Bullard. "Effect of Variable-Speed Fans on Refrigerator Component Heat Transfer." ASHRAE Transactions, Vol. 101, Part 2, 1218-1224, 1995.

Day, James and Heinz Jaster. "Refrigeration System and Refrigerant Flow Control Apparatus Therefor." U.S. Patent 5,228,308. July 1993.

Hamm, Eric K. "Design, Construction, and Evaluation of a Domestic Household Refrigerator, Environmental Test Chamber," Air Conditioning and Refrigeration Center Technical Report-13. University of Illinois at Urbana-Champaign, 1994.

Inan, Cemil. "Heat and Mass Transfer through a Domestic Refrigerator and Evaluation of Evaporator Performance Under Frosted Conditions." Ph.D. thesis. Istanbul Technical University, 2000.

Jaster, Heinz. "Refrigerator System With Dual Evaporators for Household Refrigerators." U.S, Patent 4,910,972. March 1990a.

Jaster, Heinz. "Refrigerator System With Dual Evaporators and Suction Line Heating." U.S, Patent 4,918,942. April 1990b.

Jung, D. S. and R. Radermacher. "Performance Simulation of a Two-Evaporator Refrigerator-Freezer Charged with Pure and Mixed Refrigerants," International Journal of Refrigeration-Revue Internationale du Froid, Vol.14, 254-263, 1991.

Kim, Kwangil, Bill Kopko, and Reinhard Radermacher. "Application of Tandem system to High-Efficiency Refrigerator/Freezer." ASHRAE Transactions, Vol. 101, Part 2, 1239-1247, 1995a.

Kim, Kwangil, Bill Kopko, and Reinhard Radermacher. "Tandem System Domestic Refrigerator/Freezer." Proceedings of the International Appliance Technical Conference, Urbana-Champaign, IL., May 15-17, 1995b.

Lavanis, Mahesh, Imam Haider, and Reinhard Radermacher. "Experimental Investigation of an Alternating Duty Refrigerator/Freezer," ASHRAE Transactions, Vol. 104, Part 2, 1103-1111, 1998.

Lee, H. M., H. W. Lee, and J. H. Lim. "High Efficiency Multi-Evaporator Cycle and Control of a Refrigerator." Proceedings of the International Appliance Technical Conference, West Lafayette, IN., 1996.

Liu, Y. and C. W. Bullard. "An experimental and Theoretical Analysis of Capillary Tube-Suction Line Heat Exchangers." Air Conditioning and Refrigeration Center Technical Report-109. University of Illinois at Urbana-Champaign, 1996.

Mullen , Casey. "ACRC Solver Program Listing." Air Conditioning and Refrigeration Center Technical Report-15. University of Illinois at Urbana-Champaign, 1994.

Rose, R. J., D. Jung, and R. Radermacher. "Testing of Domestic Two-Evaporator Refrigerators with Zeotropic Refrigerant Mixtures," ASHRAE Transactions, Vol. 98, Part 2, 216-225, 1992.

Samsung Website. http://samsungelectronics.com/products/refrigerator/fd_twin.html

Simmons, Kevin E., Imam Haider, and Reinhard Radermacher. "Independent Compartment Temperature Control of Lorenz-Meutzner and Modified Lorenz-Meutzner Cycle Refrigerators." ASHRAE Transactions, Vol. 102, Part1, 1085-1092, 1996

Smith, M. K., M. C. Heun, R. R. Crawford, and T. A. Newell. "Thermodynamic Performance Limit Considerations for a Dual-Evaporator, Non-Azeotropic Refrigerant Mixture-Based Domestic Refrigerator-Freezer System," International Journal of Refrigeration-Revue Internationale du Froid, Vol. 13, 237-242, July 1990.

Smith, Mark K. "Analysis and Optimization of a Dual-Load Vapor Compression Cycle Using Non-Azeotropic Refrigerant Mixtures," Ph.D. thesis. University of Illinois at Urbana-Champaign, 1994.

Srichai, P. R., and C. W. Bullard. "Two-Speed Compressor Operation in a Refrigerator/Freezer." Air Conditioning and Refrigeration Center Technical Report-121. University of Illinois at Urbana-Champaign, July 1997.

Stein, Mark A. "Moisture Transport, Frost Visualization, and Dual Evaporator Modeling in Domestic Refrigerators," MS thesis. University of Illinois at Urbana-Champaign, 1999.

Topping, Richard F. and W. David Lee. "Development of a High Efficiency, Automatic Defrosting Refrigerator-Freezer," ASHRAE Transactions, Vol. 87, Part 2, 859-867, 1982.

Won, S., D. Jung, and R. Radermacher. "An Experimental study of the Performance of Dual-Loop Refrigerator/Freezer System," International Journal of Refrigeration-Revue Internationale du Froid, Vol. 17, 411-416, July 1994.

Woodall, R. J. and C. W. Bullard. "Development, Validation, and Application of a Refrigerator Simulation Model, " Air Conditioning and Refrigeration Center Technical Report-99. University of Illinois at Urbana-Champaign, 1996.

Appendix A: Instrumentation of Prototypes

A.1 Introduction

The dual evaporator refrigerator prototypes were instrumented with thermocouples and pressure transducers in order to determine the refrigerant state at various points in its cycle. The power to the compressor and fans was measured using watt transducers.

A.2 Pressure and Thermocouple Tap Block

The pressure transducers and immersion thermocouples were connected to the refrigerant circuit with a special tap block shown in Figure A.2.1. These were fabricated from brass by the department machine shop.

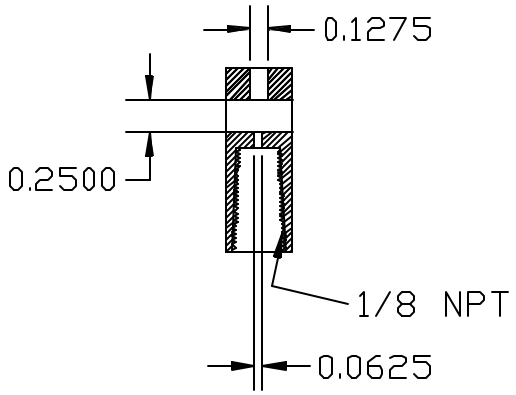

Figure A.2.1 Thermocouple Tap Block Dimensioned in Inches

To install the tap block, it is first slipped over a short (2-4 inch) piece of ¼ inch outside diameter tubing. The block is then soft soldered to the tube. The 0.125 inch and 0.0625 inch holes in the tap block are extended through the tube walls with a drill. By repeatedly inserting wires or rods through the holes and tube the drilling burrs are broken off and removed. A commercial thermocouple port (Omega part number BRLK-116-18) with a 1/8-NPT thread on one end and a .0625-inch compression fitting on the other is then screwed into the tap block. The 1/8-NPT thread is soldered to ensure a leak-free joint. Next, a capillary tube is soldered into the 0.125-inch port. This capillary tube is for connection to a pressure transducer and can be made as long as is desired and reasonable. The immersion thermocouple is then inserted into the compression fitting and the fitting is loosely tightened by hand. The tip of the thermocouple is adjusted until it is in the center of the flow and a mark is made on the thermocouple body at the point where it enters the compression fitting. The thermocouple is removed so that it will not be damaged by heat during the next step.

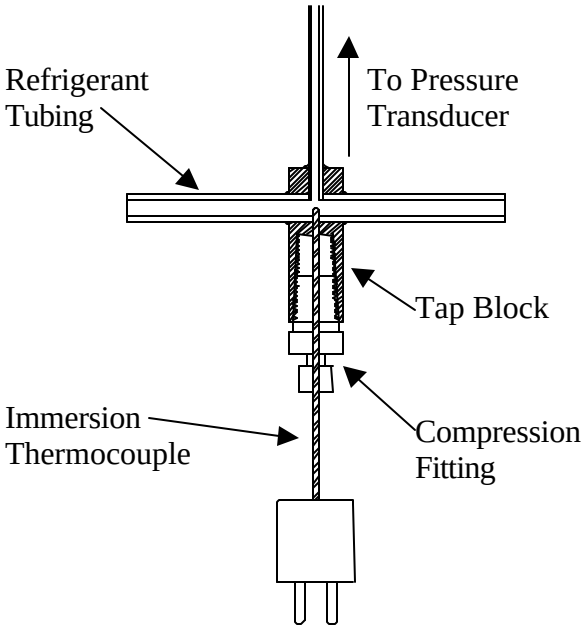

Figure A.2.2 Schematic of Tap Block Installed

Next, the tap block is soldered into the refrigerant circuit using standard soldered couplings. The capillary tube must be on the top side of the tube when installed. It must also continuously be sloped up. If it falls and then rises, the low point may fill with oil or liquid refrigerant. This would act as a manometer and give an offset to the reading. The thermocouple is reinserted so that the mark matches the end of the compression fitting when finger-tightened. The compression fitting is then tightened approximately one and a half turns. A schematic of the assembled tap block is shown in Figure A.2.2 and a photograph of the block installed at the capillary tube exit is shown in Figure A.2.3.

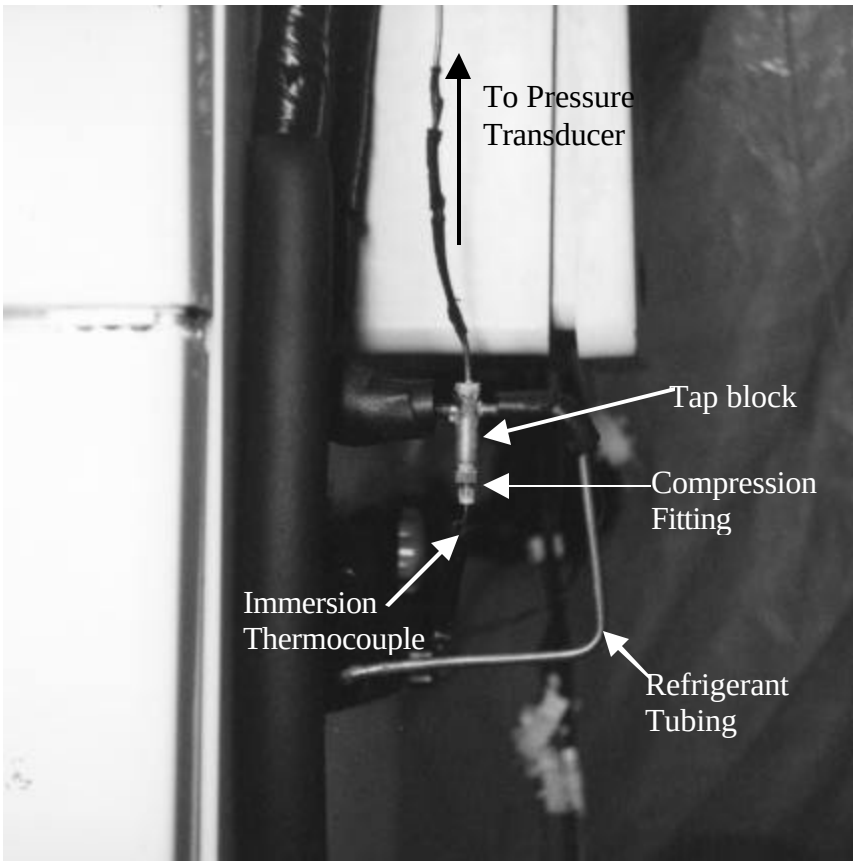

Figure A.2.3 Photograph of Tap Block Installed

A.3 Pressure Instrumentation

The pressures at six locations in the refrigerator were measured with a combination of absolute and gauge pressure transducers(see Figure A.3.1). The pressures at the compressor and condenser outlets were measured using Setra C280E transducers with a range of 0-500 psia. A Haenii ED 510/474.411/105 transducer with a calibrated range of 0-30 bars gauge was located at the condenser inlet. A Setra 207 pressure transducer with a 0-250 psig range and a Setra C280E with a 0-100 psia range were located at the fresh food evaporator exit and the freezer evaporator exit respectively. A Haenii ED 510/444.411/075 with a calibrated range of 0-30 bars gauge measured the pressure at the capillary tube exit. The technique used to calibrate the pressure transducers is described in Appendix B.

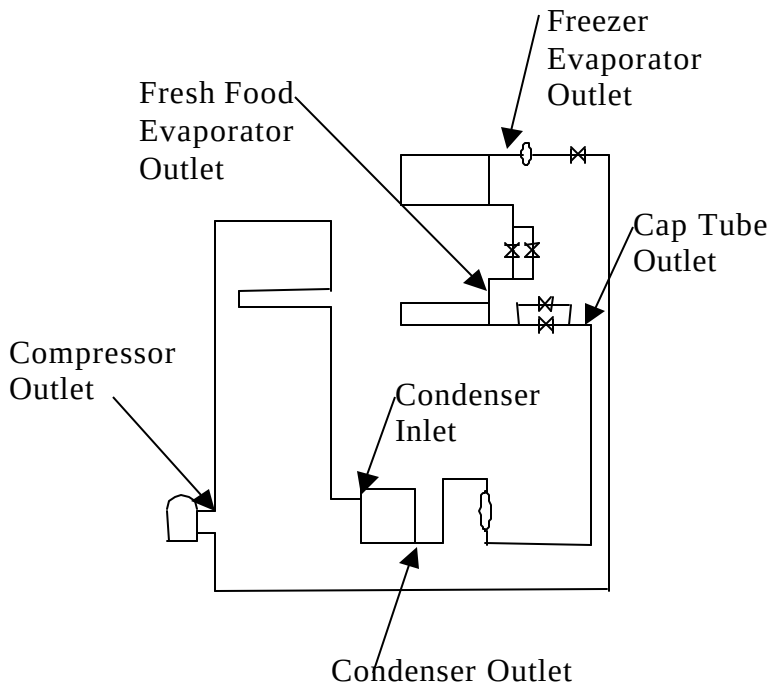

Figure A.3.1 Locations of Pressure Transducers

A.4 Thermocouples

Three main types of thermocouples were used in testing; immersion, surface and air. Ungrounded 0.625-inch diameter type T immersion thermocouples (Omega part #GTMQSS-062U-6) were connected as described above. Surface thermocouples were made of 24 gauge type T wire with a welded junction. They were then glued to the refrigerant tubing with thermally conductive epoxy and insulated with foam tape. The locations of the immersion and surface thermocouples are listed below and shown in Figure A.4.1.

A.4.1 Immersion Thermocouples

1. compressor outlet and flange heater inlet
2. flange heater outlet and condenser inlet
3. condenser outlet and cap tube inlet
4. after cap tube outlet and before pressure drop needle valve and fresh food evaporator inlet
5. after fresh food evaporator outlet and before pressure drop needle valve between evaporators
6. after pressure drop needle valve between evaporators and before freezer evaporator inlet
7. freezer evaporator outlet
8. compressor inlet

A.4.2 Surface Thermocouples

1. compressor shell top
2. compressor shell in the center of the side facing the compressor compartment cover
3. third to last row return bend
4. condenser second to last row return bend
5. fourth from last condenser return bend
6. second from last condenser return bend
7. last condenser return bend
8. filter-dryer outlet
9. after cap tube outlet and before pressure drop needle valve and fresh food evaporator inlet
10. fresh food evaporator inlet inside cabinet
11. fresh food evaporator outlet inside cabinet
12. freezer evaporator inlet inside cabinet
13. freezer evaporator outlet inside cabinet

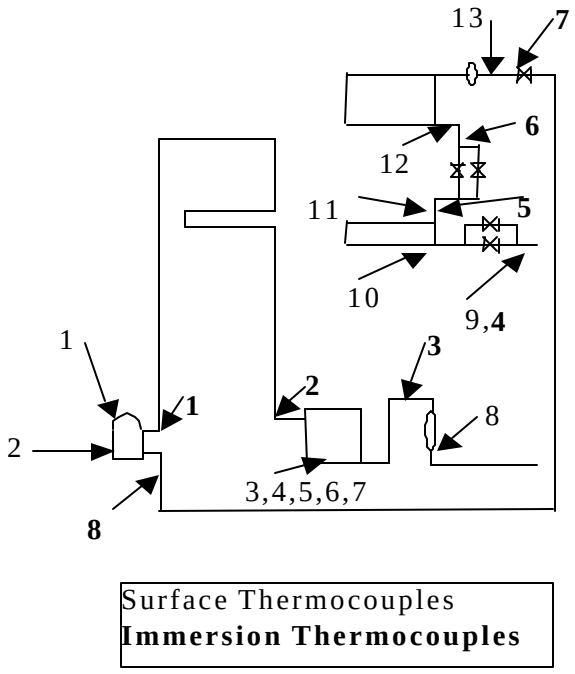

Figure A.4.1 Locations of Thermocouples Used for Measuring Refrigerant Temperatures

A.4.3 Air Thermocouples

The air thermocouples were identical to the surface thermocouples but were suspended so that they measured the temperature of the airflow. At certain locations the air flowed out of several openings or over a larger area than one thermocouple could measure. At these locations two or more thermocouples were connected electrically in parallel to take the average value of the air temperature. Figure A.4.2 shows the locations of air thermocouples inside the prototype cabinet. The air thermocouple locations are as follows:

1. fresh food evaporator air inlet (two connected in parallel)
2. fresh food evaporator air outlet top (two connected in parallel)
3. fresh food evaporator air outlet middle (two connected in parallel)
4. fresh food evaporator air outlet front (two connected in parallel)
5. fresh food evaporator air outlet bottom (two connected in parallel)
6. freezer evaporator air inlet (two connected in parallel)
7. freezer evaporator air outlet (two connected in parallel)
8. fresh food cabinet temperature top
9. fresh food cabinet temperature middle
10. fresh food cabinet temperature bottom (inside vegetable drawer)
11. freezer cabinet temperature top
12. freezer food cabinet temperature middle
13. freezer food cabinet temperature bottom
14. test chamber temperature (several connected in parallel)
15. condenser air inlet through compressor compartment cover (three connected in parallel)
16. condenser air inlet from the bottom of the refrigerator
17. condenser fan air out
18. condenser compartment air outlet (three connected in parallel)

A.4.4 Other Thermocouples

In addition, two special thermocouples were used. One was placed inside a brass slug in the middle of the fresh food compartment and is described in more detail in the chapter on performance tests. The other was inside of a simulated meat package located on the shelf directly above the vegetable drawers.

A.5 Watt Transducers

The power consumption of the refrigerator was measured using watt transducers. The power consumption of the compressor was measured using an Ohio Semitronics GW5-001X5 watt transducer. The fresh food and freezer fan power consumptions were measured separately with an Ohio Semitronics GW5-001X5 and a Scientific Columbus XC5C5A2 watt transducers. The condenser fan power was measured once and assumed to be constant for all other tests. Since the defrost heaters were not used in the tests their power consumption was not measured.

A.6 Data Acquisition System

The data acquisition system used was a Hewlett-Packard data logger connected to a Cyrix MII 300 MHz PC running HPVEE 3.2 software. The system has 48 thermocouple channels and 16 voltage channels for measuring the pressure and watt transducer outputs. A virtually identical system except for the number thermocouple of channels is described in detail in Stein (1999).

Appendix B: In Situ Pressure Transducer Calibration, Thermocouple Accuracy, and Watt Transducer Calibration

B.1 Introduction

In order to ensure the accuracy of the system measurements the pressure transducers were calibrated and the precision of the thermocouples was measured.

B.2 In Situ Pressure Transducer Calibration

B.2.1 Reasoning Behind Technique

Because the dead weight pressure calibrator normally used was broken an alternative technique was developed. A set of six Haenni pressure transducers that had previously been calibrated were selected as the reference standard. Of these three were low range (0-10 bars) and three were high range (0-30 bars).

The pressure transducers were calibrated while attached to the refrigerator and data acquisition system. Thus the effects of the data acquisition system and experimental setup were included in the calibration. However, the output readings from the pre-calibrated transducers used as a reference were assumed to be accurately read by the data acquisition system.

B.2.2 Calibration Procedure

The instrumented refrigerator was placed in the temperature controlled test chamber and allowed to sit until it uniformly reached the test chamber temperature. All calibrations were run at a nominal test chamber temperature of 25°C. During calibration of the high pressure transducers, the low side transducers were replaced with plugs in order to prevent damage by over pressure. For low side transducer calibration all transducers were installed. The system was connected to the power supplies and data acquisition system. Then the refrigerant circuit was evacuated with a vacuum pump. The pump was run for several hours to remove the R-134a dissolved in the compressor oil. Any refrigerant remaining in the system would affect the pressure readings by evaporating, condensing, and dissolving or escaping from solution in the oil.

The system was charged with dry nitrogen from a tank. The system was charged to levels of 20, 40, 60, and 80 psig as measured by the tank regulator gauge. Each of these levels was run as a separate test. After charging the data acquisition system was turned on and the voltage output from all installed transducers was recorded every 10 seconds. The tests were run for 30 minutes to an hour to ensure that the nitrogen had distributed itself through out the system uniformly. After completion of one test the system was charged to the next pressure level and the procedure repeated.

During the tests the pressure would drop slowly over time (Figure B.2.2.1). Initially this appeared to be due to a leak. However, after extensive searching no leak was found. This pressure drop is probably due to the nitrogen slowly dissolving into the compressor oil. No published data on the solubility of nitrogen in refrigerator oils was available so this effect could not be modeled.

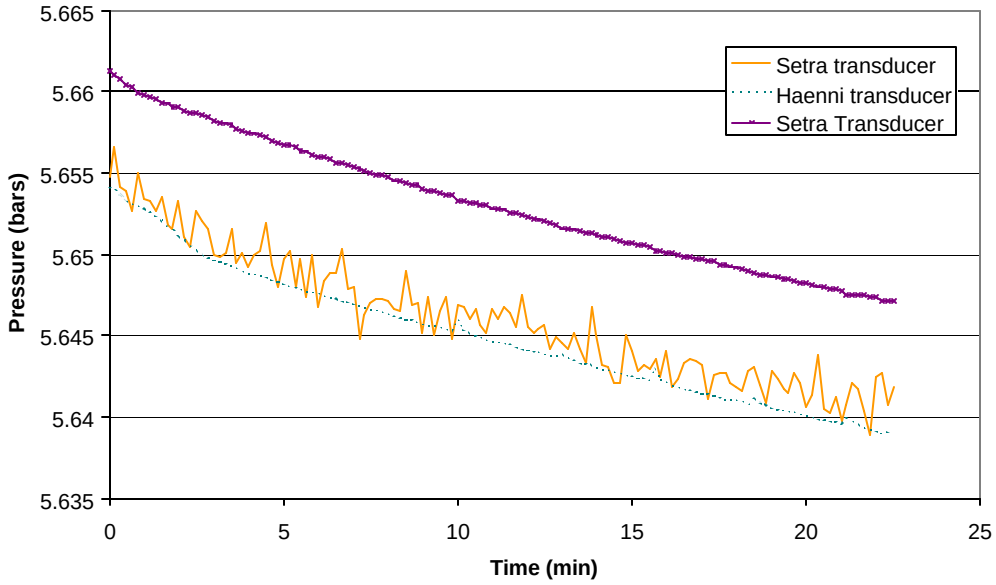

Figure B.2.2.1 Time Dependent Drop in Pressure During Calibration (80 psi Nominal Test)

After all tests were run, the voltage outputs from the last 1.5 minutes of each run were averaged. The calibration curves provided for the Haenni transducers were used to calculate the actual pressure in the system for each test. Then these pressures were plotted against the voltage output for each transducer (Figure B.2.2.2). A linear curve fit was computed using a least squares method. This was the calibration curve used in subsequent tests.

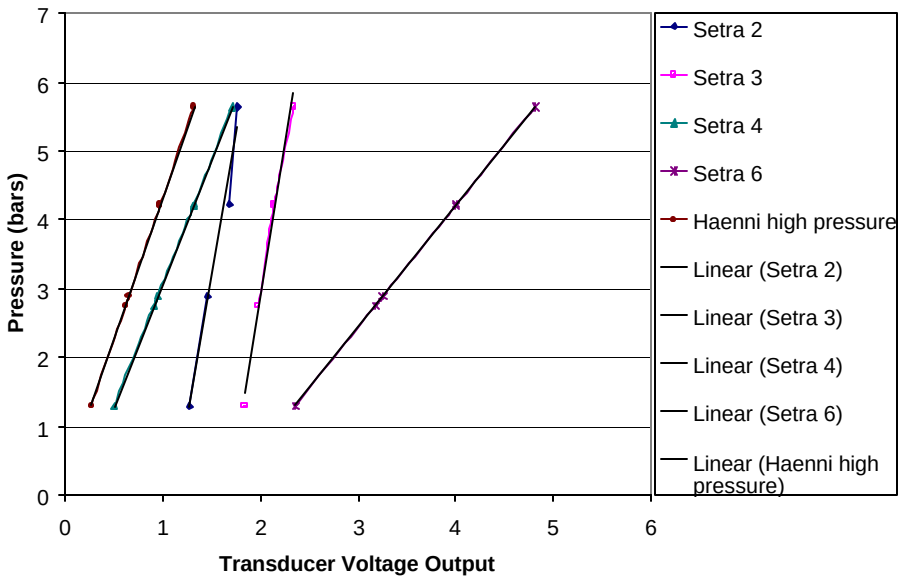

Figure B.2.2.2 Pressure Transducer Calibration Curves

All the transducers appear to be very linear over the range tested. Additional tests were performed to determine the performance of the low side pressure transducers below atmospheric pressure. The output is shown in

Figure B.2.2.3. Although one transducer bottoms out at -0.04 bars gauge, all transducers perform properly in the range encountered on the low pressure side of a refrigerator.

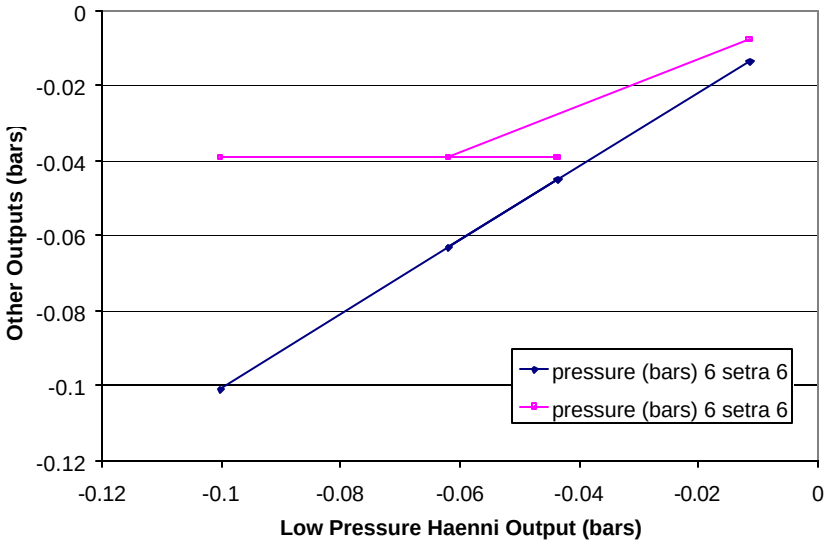

Figure B.2.2.3 Pressure Transducer Behavior Below Ambient Pressure

B.3 Thermocouple Accuracy

To determine the precision of the thermocouples, the refrigerator was left in the test chamber with the chamber door closed overnight. The fresh food and freezer doors of the refrigerator were left open. The test chamber was left off. This allowed the whole system to come to thermal equilibrium with its surroundings. Then the temperature readings from all of the thermocouples were recorded every 10 seconds for a period of 1-3 hours to ensure that the temperatures remained steady. The temperature from each thermocouple was averaged over the last 100 data points in each test. These averages were then averaged to make an overall average.

Initially it was expected that offset values could be determined by subtracting the individual averages from the overall average offset values could be determined. By adding these offset values to the readings the bias error of the temperature measurements could be decreased. However, the thermocouple readings increase with their height on the refrigerator (Figure B.3.1). This indicates that the air in the test chamber is thermally stratified. This actual variation in temperature accounts for much of the variation between thermocouple readings.

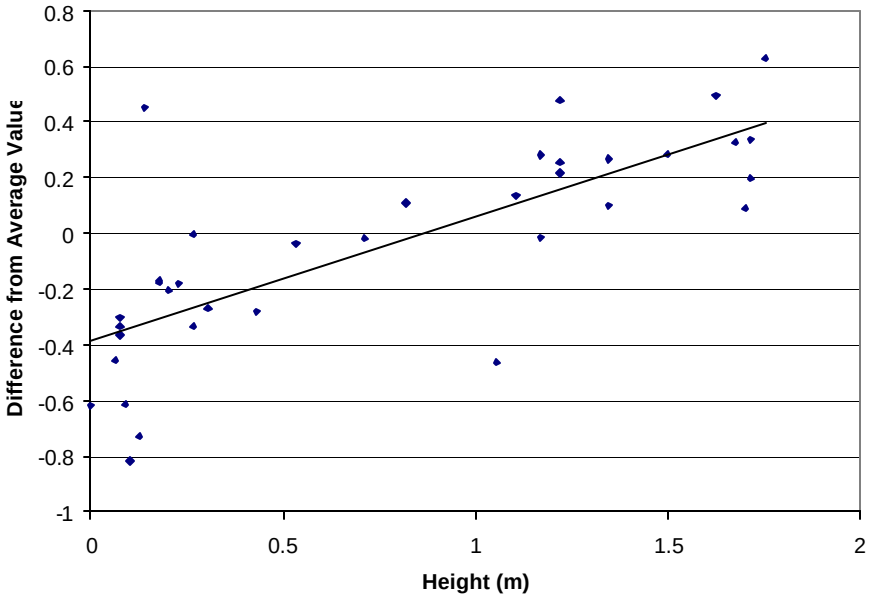

Figure B.3.1 Increase in Thermocouple Readings With Height on Refrigerator

The average value for each type of thermocouple (immersion, surface, and air) differed from the overall average less than the standard deviations of the readings with in each group. Therefore it appears that there is no significant difference in readings from each thermocouple type.

Similar tests had been run with the test chamber on and actively controlling the temperature inside. However, variations in the thermocouple readings were not repeatable between tests. In addition cooler temperatures in one region of the refrigerator were due to cold air blowing from the test chamber climate control system. Therefore this data was not quantitatively useful, but did demonstrate the difficulties involved in determining thermocouple offset values.

Because it was unclear in the later tests whether the variation between the thermocouple readings was due to inaccuracies in the thermocouples or to actual temperature variations no adjustment was made to the temperature measurements.

B.4 Watt Transducer Calibration

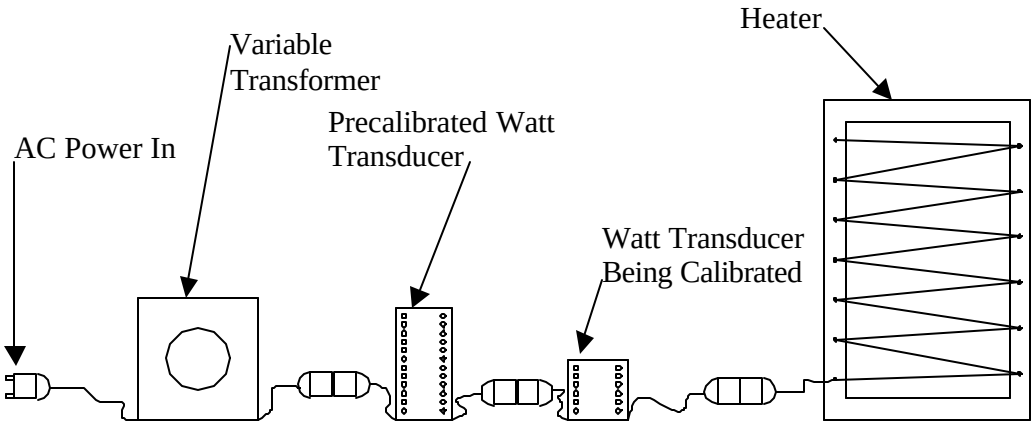

Figure B.4.1 Watt Transducer Calibration Setup

The watt transducers were calibrated with respect to a Ohio Semitronics GH-002C-P-50 watt transducer that had been calibrated in an off campus laboratory. The transducer being calibrated was attached in series with the precalibrated transducer. It was then attached to one of the resistance heaters as a load and a variable transformer, variac, as a source (Figure B.4.1). The variac was turned on and the voltage output from both transducers was read by the data acquisition system. The variac was then set to a different voltage and the next reading taken. The voltages read from the precalibrated transducer were used to determine the actual power. The output from the transducer being calibrated was then used to make a linear curve fit with the power. All transducers calibrated were very linear and varied only slightly from the nominal calibration.

Appendix C: XK File Description

Mode			**Variable Name**	**Description**	***Units***
fitting	kitchen	lab			
K	K	K	Acond	Air-side area of the condenser	[ft^2]
K	K	K	Aevap	Air-side area of the freezer evaporator	[ft^2]
X	X	X	CaCond	Heat capacity of the condenser air stream	[Btu/hr-F]
X	X	X	CaEvap	Heat capacity of the freezer evaporator air stream	[Btu/hr-F]
X	X	X	COP	Coefficient of performance	[ ]
X	X	X	DpDischarge	Pressure drop in the discharge line	[psia]
X	X	X	DpSupCond	Pressure drop in the superheated zone of condenser	[psia]
X	X	X	Dp2phCond	Pressure drop in the two-phase zone condenser	[psia]
X	X	X	DpSubCond	Pressure drop in the subcooled zone condenser	[psia]
X	X	X	DpLiquid	Pressure drop in the liquid line	[psia]
X	X	X	Dp2phEvap	Pressure drop in the two-phase zone evaporator	[psia]
X	X	X	DpSupEvap	Pressure drop in the superheated zone evaporator	[psia]
X	X	X	DpSuction	Pressure drop in the suction line	[psia]
X	X	X	DPin	Pressure steps in inlet capillary tube section	[psia]
X	X	X	DPout	Pressure steps in outlet capillary tube secion	[psia]
X	X	X	DTsl	Temperature steps in suction line heat exchanger	[F]
X	X	X	Energy	Steady-state energy usage for the entire year	[kW-hr/yr]
X	X	X	fsubcond	Fraction of subcooled portion of the condenser	[ ]
X	X	X	f2phcond	Fraction of two-phase portion of the condenser	[ ]
X	X	X	fsupcond	Fraction of superheated portion of the condenser	[ ]
X	X	X	f2phevap	Fraction of two-phase portion of the evaporator	[ ]

X	X	X	fsupevap	Fraction of superheated portion of the evaporator	[ ]
X	X	X	h0	Specific enthalpy at the compressor outlet	[Btu/lbm]
X	X	X	h1	Specific enthalpy at the condenser inlet	[Btu/lbm]
X	X	X	h21	Specific enthalpy at x=1.0 of condenser	[Btu/lbm]
X	X	X	h20	Specific enthalpy at x=0.0 of condenser	[Btu/lbm]
X	X	X	h3	Specific enthalpy at the condenser exit	[Btu/lbm]
X	X	X	h4	Specific enthalpy at the captube inlet	[Btu/lbm]
X	X	X	hcrit	Specific enthalpy at the exit of capillary tube	[Btu/lbm]
X	X	X	h8	Specific enthalpy at the inlet to the freezer evaporator	[Btu/lbm]
X	X	X	h81	Specific enthalpy at x=1.0 in the freezer evaporator	[Btu/lbm]
X	X	X	h9	Specific enthalpy at the exit of the freezer evaporator	[Btu/lbm]
X	X	X	h11	Specific enthalpy at the compressor inlet	[Btu/lbm]
X	X	X	MDisLine	Mass of refrigerant in the discharge line	[lbm]
X	X	X	MCond	Mass of refrigerant in the condenser	[lbm]
X	X	X	MLiqLine	Mass of refrigerant in the liquid line	[lbm]
X	X	X	MCapTube	Mass of refrigerant in capillary tube	[lbm]
X	X	X	MEvap	Mass of refrigerant in the freezer evaporator	[lbm]
X	X	X	MSuctLine	Mass of refrigerant in suction line	[lbm]
X	X	X	MAccum	Mass of refrigerant in accumulator	[lbm]
X	X	X	MCompvap	Mass of refrigerant refrigerant vapor in compressor	[lbm]
X	X	X	MCompoil	Mass of refrigerant dissolved in the compressor oil	[lbm]

X	X	X	Mtotal	Mass of refrigerant in the entire system	[lbm]
X	X	X	p0	Refrigerant pressure at the compressor outlet	[psia]
X	X	X	p1	Refrigerant pressure at the condenser inlet	[psia]
X	X	X	p21	Refrigerant pressure at x=1.0 in the condenser	[psia]
X	X	X	p20	Refrigerant pressure at x=0.0 in the condenser	[psia]
X	X	X	p3	Refrigerant pressure at the condenser outlet	[psia]
X	X	X	p4	Refrigerant pressure at the capillary tube inlet	[psia]
X	X	X	pcrit	Refrigerant pressure at the capillary tube outlet	[psia]
X	X	X	p8	Refrigerant pressure at the freezer evaporator inlet	[psia]
X	X	X	p81	Refrigerant pressure at x=1.0 in the freezer evaporator	[psia]
X	X	X	p9	Refrigerant pressure at the freezer evaporator outlet	[psia]
X	X	X	p11	Refrigerant pressure at the compressor inlet	[psia]
X	X	X	powercomp	Power consumed by the compressor	[Watts]
X	X	X	qcond	Total heat transfer from the condenser	[Btu/hr]
X	X	X	qsupcond	Heat transfer from the superheated condenser zone	[Btu/hr]
X	X	X	q2phcond	Heat transfer from the two-phase condenser zone	[Btu/hr]
X	X	X	qsubcond	Heat transfer from the subcooled condenser zone	[Btu/hr]
X	X	X	qevap	Total heat transfer to the freezer evaporator	[Btu/hr]
X	X	X	q2phevap	Heat transfer from the two-phase evaporator zone	[Btu/hr]
X	X	X	qsupevap	Heat transfer from the superheated evaporator zone	[Btu/hr]
X	X	X	qcomp	Heat transfer from the condenser	[Btu/hr]

X	X	X	Qfrez	Total heat input to the freezer compartment	[Btu/hr]
X	X	X	Qfrig	Total heat input to the fresh food compartment	[Btu/hr]
X	X	K	RunTime	Ratio of the total system load to the system capacity	[ ]
X	X	X	t0	Refrigerant temperature at the compressor outlet	[F]
X	X	X	t1	Refrigerant temperature at the condenser inlet	[F]
X	X	X	t21	Refrigerant temperature at x=1.0 in the condenser	[F]
X	X	X	t20	Refrigerant temperature at x=0.0 in the condenser	[F]
X	X	X	t3	Refrigerant temperature at the condenser outlet	[F]
X	X	X	t4	Refrigerant temperature at the capillary tube inlet	[F]
X	X	X	tcrit	Refrigerant temperature at the capillary tube outlet	[F]
X	X	X	t8	Refrigerant temperature at the freezer evaporator inlet	[F]
X	X	X	t81	Refrigerant temperature at x=1.0 in the freezer evaporator	[F]
X	X	X	t9	Refrigerant temperature at the freezer evaporator outlet	[F]
X	X	X	t11	Refrigerant temperature at the compressor inlet	[F]
X	X	X	Tsat0	Saturation temperature at p0 (for compressor map)	[F]
X	X	X	Tsat11	Saturation temperature at p11 (for compressor map)	[F]
X	X	X	tacondin	Air temperature at condenser inlet	[F]
X	X	X	tacondout	Air temperature at condenser outlet	[F]
X	X	X	tacondfanin	Air temperature at the condenser fan inlet	[F]
X	X	X	tacondfanout	Air temperature at the condenser fan outlet	[F]
X	X	X	taevapin	Air temperature at the freezer evaporator inlet	[F]

X	X	X	taevapmid	Air temperature in between the parallel-flow two-phase zone and the superheated zone in the evaporator	[F]
X	X	X	taevapout	Air temperature at the freezer evaporator outlet/fan inlet	[F]
X	X	X	taevapfanout	Air temperature at the freezer evaporator fan outlet	[F]
X	X	X	usupcond	Overall heat transfer coefficient for superheated zone of the condenser	[Btu/hr-ft^2-F]
X	X	X	u2phcond	Overall heat transfer coefficient for two-phase zone of the condenser	[Btu/hr-ft^2-F]
X	X	X	usubcond	Overall heat transfer coefficient for subcooled zone of the condenser	[Btu/hr-ft^2-F]
X	X	X	u2phevap	Overall heat transfer coefficient for two-phase zone of the evaporator	[Btu/hr-ft^2-F]
X	X	X	usupevap	Overall heat transfer coefficient for superheated zone of the evaporator	[Btu/hr-ft^2-F]
X	X	X	v0	Refrigerant volume at the compressor outlet	[ft^3/lbm]
X	X	X	v1	Refrigerant volume at the condenser inlet	[ft^3/lbm]
X	X	X	v21	Refrigerant volume at x=1.0 in the condenser	[ft^3/lbm]
X	X	X	v20	Refrigerant volume at x=0.0 in the condenser	[ft^3/lbm]
X	X	X	v3	Refrigerant volume at the condenser outlet	[ft^3/lbm]
X	X	X	v4	Refrigerant volume at the capillary tube inlet	[ft^3/lbm]
X	X	X	vcrit	Refrigerant volume at the capillary tube outlet	[ft^3/lbm]
X	X	X	v80	Refrigerant volume at x=0.0 in the freezer evaporator	[ft^3/lbm]
X	X	X	v8	Refrigerant volume at the freezer evaporator inlet	[ft^3/lbm]
X	X	X	v71	Refrigerant volume at x=1.0 in the freezer evaporator	[ft^3/lbm]

X	X	X	v9	Refrigerant volume at the freezer evaporator outlet	[ft^3/lbm]
X	X	X	v11	Refrigerant volume at the compressor inlet	[ft^3/lbm]
X	X	X	w	Refrigerant mass flow rate	[lbm/hr]
X	X	X	Woil	Mass fraction of refrigerant in oil/refrig. mixture	[ ]
X	X	X	xcrit	Refrigerant quality at the capillary tube outlet	[ ]
X	X	X	xoc	Refrigerant quality at the condenser outlet	[ ]
X	X	X	x8	Refrigerant quality at the freezer evaporator inlet	[ ]
X	X	X	xoe	Refrigerant quality at the freezer evaporator outlet	[ ]
K	K	K	AAFC	Frontal air-flow area in the condenser	[ft^2]
K	K	K	AAFE	Frontal air-flow area in the freezer evaporator	[ft^2]
X	X	X	alphacond	Ratio of external to internal area in the condenser	[ ]
X	X	X	alphaevap	Ratio of external to internal area in the freezer evaporator	[ ]
K	K	K	beta_Pmap	Multiplier to scale the the compressor power map	[ ]
K	K	K	beta_wmap	Multiplier to scale the the compressor mass flow map	[ ]
K	K	K	beta_condfan	Multiplier to scale the the condenser fan speed	[ ]
K	K	K	beta_evapfan	Multiplier to scale the the freezer evaporator fan speed	[ ]
X	X	X	CaptubeModel	Indicates whether the captube model is used 'K' = the capillary tube model will be used 'X' = the capillary tube model will not be used	[ ]
K	K	K	CaptubeOutput	Indicates the amount of captube model output 0 = No output 1 = Captube variable profile at the final solution 2 = Captube variable profile every iteration	[ ]
K	K	K	CompNum	Compressor map to be used by the model	[ ]

K	K	K	crtmult	Multiplier for the refrigerant-side heat transfer correlation in the condenser to simulate microfinned tubing	[ ]
K	K	K	Ddisline	Inside diameter of the discharge line	[ft]
K	K	K	Dcond	Inside diameter of the condenser tubing	[ft]
K	K	K	Dliqline	Inside diameter of the liquid line	[ft]
K	K	K	Dct	Inside diameter of the capillary tube	[ft]
K	K	K	Devap	Inside diameter of the freezer evaporator tubing	[ft]
C	C	C	Dsuctline	Inside diameter of the suction line	[ft]
K	K	K	DZC	Total straight tube length in the condenser	[ft]
K	K	K	DZE	Total straight tube length in the freezer evaporator	[ft]
K	K	K	ertmult	Multiplier for the refrigerant-side heat transfer correlation in the evaporator to simulate microfinned tubing	[ ]
K	K	K	ectslhx	Effectiveness of the captube-suction line heat heat exchanger (calculated when the captube model is used, and specified when the captube model is not)	[ ]
K	K	K	frecirc	Fraction of the condenser exit air that recirculates back into the condenser inlet	[ ]
K	K	X	FrezHeater	Power input to the freezer compartment by the heaters(or any other source)	[Watts]
K	K	X	FrigHeater	Power input to the fresh food compartment by the heaters (or any other source)	[Watts]
K	K	K	hAcomp	Heat transfer coefficient of the compressor shell	[Btu/hr-F]
K	K	K	haircond	Air-side heat transfer coefficient of the condenser	[Btu/hr-F]

K	K	K	hcondNum	Indicates whether haircond is specified by the user or obtained from a correlation 0 = user specified 1 & higher = correlations (See haircnd in EQNSUBS.f)	[ ]
K	K	K	hairevap	Air-side heat transfer coefficient of the freezer evaporator	[Btu/hr-F]
K	K	K	hevapNum	Indicates whether hairevap is specified by the user or obtained from a correlation 0 = user specified 1 & higher = correlations (See hairevp in EQNSUBS.f)	[ ]
K	K	K	K1oil	Coefficient for refrigerant-oil mixture solubility	[ ]
K	K	K	K2oil	Coefficient for refrigerant-oil mixture solubility	[ ]
K	K	K	K3oil	Coefficient for refrigerant-oil mixture solubility	[ ]
K	K	K	K4oil	Coefficient for refrigerant-oil mixture solubility	[ ]
K	K	K	K5oil	Coefficient for refrigerant-oil mixture solubility	[ ]
K	K	K	K6oil	Coefficient for refrigerant-oil mixture solubility	[ ]
K	K	K	K7oil	Coefficient for refrigerant-oil mixture solubility	[ ]
K	K	K	Ldisline	Length of discharge line	[ft]
K	K	K	Lcond	Total length of condenser tubing (w/ return bends)	[ft]
K	K	K	Lliqline	Length of liquid line	[ft]
K	K	K	Lin	Length of adiabatic inlet section of capillary tube	[ft]
K	K	K	Lhx	Length of the captube-suction line heat exchanger	[ft]
K	K	K	Lout	Length of the adiabatic outlet region of the capillary tube	[ft]
K	K	K	Levap	Total length of freezer evaporator tubing (w/ return bends)	[ft]
K	K	K	Lsuctline	Length of the suction line	[ft]

K	K	K	Moil	Mass of oil in the compressor sump	[lbm]
K	K	K	NSECTC	Number of equivalent circuits in the condenser	[ ]
K	K	K	NSECTE	Number of equivalent circuits in the freezer evaporator	[ ]
K	K	K	numDPin	Number of pressure steps in the captube inlet section used in the solution process	[ ]
K	K	K	numDPout	Number of pressure steps in the captube outlet section used in the solution process	[ ]
K	K	K	numDTsl	Number of temperature steps in the suction line heat exchanger section used in the solution process	[ ]
K	K	K	patm	Atmospheric pressure	[psia]
K	K	K	pcondfan	Power used by condenser fan	[Watts]
K	K	K	pevapfan	Power used by the freezer evaporator fan	[Watts]
K	K	K	rough	Average surface roughness inside system tubing	[ft]
K	K	K	RTBCND	Number of return bends in the condenser	[ ]
K	K	K	RTBEVP	Number of return bends in the freezer evaporator	[ ]
K	K	K	subcool	Degrees of subcooling at the condenser exit	[F]
K	K	K	superheat	Degrees of superheating at the freezer evaporator exit	[F]
K	K	K	STC	Spacing between tubes in the condenser (return bend diameter)	[ft]
K	K	K	STE	Spacing between tubes in the freezer evaporator (return bend diameter)	[ft]
K	K	K	tamb	Ambient room temperature	[F]
X	K	K	tafrig	Average air temperature in the fresh food compartment	[F]
K	K	K	tafrez	Average air temperature in the freezer compartment	[F]

K	K	K	UAf	Overall heat transfer coefficient for the freezer section of the refrigerator "box"	[W/F]
K	K	K	UAz	Overall heat transfer coefficient for the fresh food section of the refrigerator "box"	[W/F]
K	K	K	vdotcond	Volumetric air flow rate through the condenser	[ft^3/min]
K	K	K	vdotevap	Volumetric air flow rate through the freezer evaporator	[ft^3/min]
K	K	K	volfilter	Internal free volume of the filter drier	[ft^3]
K	K	K	volaccum	Internal volume of the accumulator (if any)	[ft^3]
K	K	K	volcomp	Internal free vapor volume of the compressor	[ft^3]
C	C	C	Cooling	Availability, or exergy, delivered to the cold space by the refrigeration system	[Btu/hr]
C	C	C	Itot	Total irreversibility, or destroyed exergy, in the system	[Btu/hr]
C	C	C	Icomp	Total irreversibility, or destroyed exergy, in the compressor	[Btu/hr]
C	C	C	Icond	Total irreversibility, or destroyed exergy, in the condenser	[Btu/hr]
C	C	C	Ievap	Total irreversibility, or destroyed exergy, in the freezer evaporator	[Btu/hr]
C	C	C	Ipipes	Total irreversibility, or destroyed exergy, in the rest of the tubing	[Btu/hr]
C	C	C	pcondfan_calc	Calculated condenser fan power based on the fan laws and beta_condfan	[Watts]
C	C	C	pevapfan_calc	Calculated condenser fan power based on the fan laws and beta_evapfan	[Watts]
C	C	C	TcondAvg	Average two-phase condensing temperature	[F]

C	C	C	TevapAvg	Average two-phase evaporating temperature	[F]
C	C	C	vdotcond_calc	Calculated condenser volumetric air flow rate based on the fan laws and beta_condfan	[ft^3/min]
C	C	C	vdotevap_calc	Calculated freezer evaporator volumetric air flow rate based on the fan laws and beta_evapfan	[ft^3/min]
C	C	C	voldisline	Internal volume of the discharge line	[ft^3]
C	C	C	Volcond	Internal volume of the condenser	[ft^3]
C	C	C	volliqline	Internal volume of the liquid line	[ft^3]
C	C	C	volcaptube	Internal volume of the capillary tube	[ft^3]
C	C	C	Volevap	Internal volume of the freezer evaporator	[ft^3]
C	C	C	volsuctline	Internal volume of the suction line	[ft^3]
X	X	X	xoll	Refrigerant quality at the liquid line outlet	[ ]
X	X	X	subcool_liq	Degrees of subcooling at the liquid line	[F]
X	X	X	qliqlinef	Heat transfer in the liquid line section next to the fresh food compartment	[Btu/hr]
K	K	K	Lt	Length of each condenser tube	[ft]
K	K	K	Nt	Number of condenser tubes	[ ]
K	K	K	Dw	Diameter of the condenser wires	[ft]
K	K	K	Sw	Wire spacing in the condenser	[ft]
K	K	K	Lw	Length of each condenser wire	[ft]
K	K	K	Nw	Number of condenser wires	[ ]
K	K	K	psi	Angle between air flow direction and condenser wires (0 degrees perpendicular to wires)	[degrees]
K	K	K	alpha	Angle of attack of condenser	[degrees]
X	X	X	DpCond	Total pressure drop in the condenser	[psia]
X	X	X	DpEvap	Total pressure drop in the freezer evaporator	[psia]

K	K	K	UAliqline	Overall heat transfer coefficient for the liquid line	[Btu/hr-F]
K	K	K	Cap_clog	Fraction of the capillary tube exit that is open (used to simulate capillary tube clogging by reducing exit area)	[ ]
K	K	K	AAFEf	Frontal air-flow area in the fresh food evaporator	[ft^2]
K	K	K	Aevapf	Air-side area of the fresh food evaporator	[ft^2]
X	X	X	alphaevapf	Ratio of external to internal area in the fresh food evaporator	[ ]
X	X	X	CaEvapf	Heat capacity of the fresh food evaporator air stream	[Btu/hr-F]
K	K	K	Devapf	Inside diameter of the evaporator tubing	[ft]
K	K	K	DpBetweenEvap	The pressure drop between the evaporators	[psia]
X	X	X	DpEvapf	Total pressure drop in the fresh food evaporator	[psia]
K	K	K	DZEf	Total straight tube length in the fresh food evaporator	[ft]
X	X	X	h7	Specific enthalpy at the inlet to the fresh food evaporator	[Btu/lbm]
X	X	X	h71	Specific enthalpy at x=1.0 in the fresh food evaporator	[Btu/lbm]
K	K	K	hairevapf	Air-side heat transfer coefficient of the fresh food evaporator	[Btu/hr-F]
K	K	K	hevapfNum	Indicates whether hairevapf is specified by the user or obtained from a correlation 0 = user specified 1 & higher = correlations (See hairevp in EQNSUBS.f)	[ ]
C	C	C	Ievapf	Total irreversibility, or destroyed exergy, in the fresh food evaporator	[Btu/hr]
K	K	K	Levapf	Total length of evaporator tubing (w/ return bends)	[ft]
X	X	X	MEvapf	Mass of refrigerant in the fresh food evaporator	[lbm]

K	K	K	NSECTEf	Number of equivalent circuits in the fresh food evaporator	[ ]
X	X	X	p7	Refrigerant pressure at the fresh food evaporator inlet	[psia]
X	X	X	p79	Refrigerant pressure at the fresh food evaporator outlet	[psia]
K	K	K	pevapffan	Power used by the fresh food evaporator fan	[Watts]
X	X	X	qevapf	Total heat transfer to the fresh food evaporator	[Btu/hr]
K	K	K	RTBEVPf	Number of return bends in the fresh food evaporator	[ ]
K	K	K	STEf	Spacing between tubes in the fresh food evaporator (return bend diameter)	[ft]
X	X	X	t7	Refrigerant temperature at the fresh food evaporator inlet	[F]
X	X	X	t71	Refrigerant temperature at x=1.0 in the fresh food evaporator	[F]
X	X	X	taevapffanout	Air temperature at the fresh food evaporator fan outlet	[F]
X	X	X	taevapfout	Air temperature at the fresh food evaporator outlet/fan inlet	[F]
K	K	K	UAm	Overall heat transfer coefficient for the mullion of the refrigerator	[W/F]
X	X	X	uevapf	Calculated value of the overall heat transfer coefficient of the fresh food evaporator	[Btu/hr-ft^2-F
X	X	X	v7	Refrigerant volume at the fresh food evaporator inlet	[ft^3/lbm]
X	X	X	v70	Refrigerant volume at x=0.0 in the fresh food evaporator	[ft^3/lbm]
X	X	X	v71	Refrigerant volume at x=1.0 in the fresh food evaporator	[ft^3/lbm]
K	K	K	vdotevapf	Volumetric air flow rate through the fresh food evaporator	[ft^3/min]
C	C	C	Volevapf	Internal volume of the fresh food evaporator	[ft^3]
X	X	X	xie	Refrigerant quality at the fresh food evaporator inlet	[ ]

K	X	K	beta_evapffan	Multiplier to scale the fresh food evaporator fan on time	[ ]
X	X	X	vdotevapf_calc	Calculated evaporator volumetric air flow rate (beta_evapfan*vdotevapf)	[ft^3/min]
X	X	X	pevapffan_calc	Power used by the fresh food evaporator fan	[Watts]
X	X	X	qliqlinez	Heat transfer in the liquid line section next to the freezer	[Btu/hr]
X	X	X	t3a	Refrigerant temperature in a post condenser loop at the point between the fresh food and freezer sections	[F]
K	K	K	flnghtratio	Fraction of the flange heater length in contact with the fresh food cabinet to it's total length	[ ]
X	X	X	h3a	Refrigerant enthalpy in a post condenser loop at the point between the fresh food and freezer sections	[Btu/lbm]
K	K	K	UAdischarge	Overall heat transfer coefficient for the discharge line	[Btu/hr-F]
X	X	X	qdischargef	Heat transfer from the discharge line next to the fresh food compartment	[Btu/hr]
X	X	X	qdischargez	Heat transfer from the discharge line next to the freezer	[Btu/hr]
X	X	X	t0a	Refrigerant temperature in the hot loop at the point between the fresh food and freezer sections	[F]
X	X	X	h0a	Refrigerant enthalpy in the discharge hot loop at the point between the fresh food and freezer sections	[Btu/lbm]

Acknowledgement: This chart is adapted from other charts by Woodall (1996) and others.

Appendix D: Code Blocks Added to RFSIM

D.1 Code Added to EQNS.f for Fan Scaling

```
C*******fan scaling equations**********************
C******Added so that beta_evapffan could be solved for as an X
2800  R(faneq+0)=vdotevapf_calc - vdotevapf*beta_evapffan
      GOTO 1

2820      R(faneq+1)=pevapffan_calc - pevapffan*(beta_evapffan)
      GOTO 1
```

Note: In all other locations in EQNS.f the variable "vdotevapffan" was changed to "vdotevapf_calc." Likewise, "pevapffan" was changed to "pevapffan_calc."

D.2 Code Added for Discharge Line and Liquid Line Flange Heaters

D.2.1 Code Modified in Main Section of EQNS.f for the Liquid Line

```
C*******Assumes that if liquid line is less than 3 ft long it is not in
C*******thermal contact with cabinet.
510   IF(Lliqline.GT.3) THEN
            LMTD_liqlinef = ((t3-tamb)-(t3a-tamb))/log((t3-tamb)/(t3a
     &   -tamb))
           ELSE
            LMTD_liqlinef=0.0
           END IF
      R(prop+25) = UAliqline * flnghtratio * LMTD_liqlinef - qliqlinef
      GOTO 1

520    R(prop+26) = p3 - p4 - DpLiquid
      GOTO 1

540    R(prop+27) = h3 - h3a - (qliqlinef)/w
      GOTO 1
```

D.2.2 Code Added after Main Section of EQNS.f

```
CCCCCCCCCCCCCCCCCCCCCCCCCCCCCCCCCCCCCCCCCCCCCCCCCCCCCCCCCCCCCCCC
C          Additional Flange Heater Equations                C
CCCCCCCCCCCCCCCCCCCCCCCCCCCCCCCCCCCCCCCCCCCCCCCCCCCCCCCCCCCCCCCC

C      These equations were added so that a refrigerant circuit that
C      heats the front flange of the refrigerator can be more fully
C      modeled.  They account for different relative lengths of the
C      heater in thermal contact with the two compartments.  In
C      addition a circuit before or after the condenser can be modeled.

2660       IF(Lliqline.GT.3) THEN
           LMTD_liqlinez = ((t3a-tamb)-(t4-tamb))/log((t3a-tamb)/(t4
     &   -tamb))
```

```
            ELSE
              LMTD_liqlinez=0.0
            END IF
     R(flnght+0) = UAliqline * (1-flnghtratio) * LMTD_liqlinez
    &   - qliqlinez
        GOTO 1

2680  R(flnght+1) = h3a - h4 - (qliqlinez)/w
      GOTO 1

2700        call TPHiter(p3*flnghtratio+(1-flnghtratio)*p4,h3a,t3atemp)
            R(flnght+2) = t3a-t3atemp
      GOTO 1
C*******Discharge line flange heater equations**********************
C*******If the discharge line is less than 3 ft it is set as adiabatic.
C*******Assumes that all heat transfer resistance is on the refrigerant side

2720  IF(Ldisline.GT.3.0) THEN
              LMTD_dischargef = ((t0-tamb)-(t0a-tamb))/log((t0-tamb)
    &    /(t0a-tamb))
            ELSE
              LMTD_dischargef=0.0
            END IF
     R(flnght+3) = UAdischarge * flnghtratio * LMTD_dischargef
    &   - qdischargef
        GOTO 1

2740        IF(Ldisline.GT.3.0) THEN
             LMTD_dischargez = ((t0a-tamb)-(t1-tamb))/log((t0a-tamb)/(t1
    &   -tamb))
            ELSE
             LMTD_dischargez=0.0
            END IF
     R(flnght+4) = UAdischarge * (1-flnghtratio) * LMTD_dischargez
    &   - qdischargez
        GOTO 1

2760  R(flnght+5) = h0a - h1 - (qdischargez)/w
      GOTO 1

2780        call TPHiter(p0*flnghtratio+(1-flnghtratio)*p1,h0a,t0atemp)
            R(flnght+6) = t0a-t0atemp
      GOTO 1
```

Appendix E: Long Fan Cycle Freezer Evaporator Exit and Compressor Exit Data

E.1 Introduction

The following graphs correspond to the description in Section 2.7.2 Effects of Fresh Food Fan Cycling on Performance and Charge Distribution. In the description in the main body of the thesis, the test with 350 gram charge and 32°C ambient temperature was used as the example. The differences between the 32°C example and the other tests are described below.

E.2 16°C Ambient Temperature 350 Gram Charge Test

In this test, the refrigerant enters the compressor as two-phase during the end of the fan-off period and through the whole on period. Since the fan-on periods are shorter there is not enough time for the refrigerant accumulated in the fresh food evaporator to boil off and allow superheat at the compressor inlet. Superheat at the inlet starts as soon as the fan turns off and the evaporator pressure drops. As the fresh food evaporator did not completely boil off the accumulated refrigerant, it quickly refills and the superheat drops off.

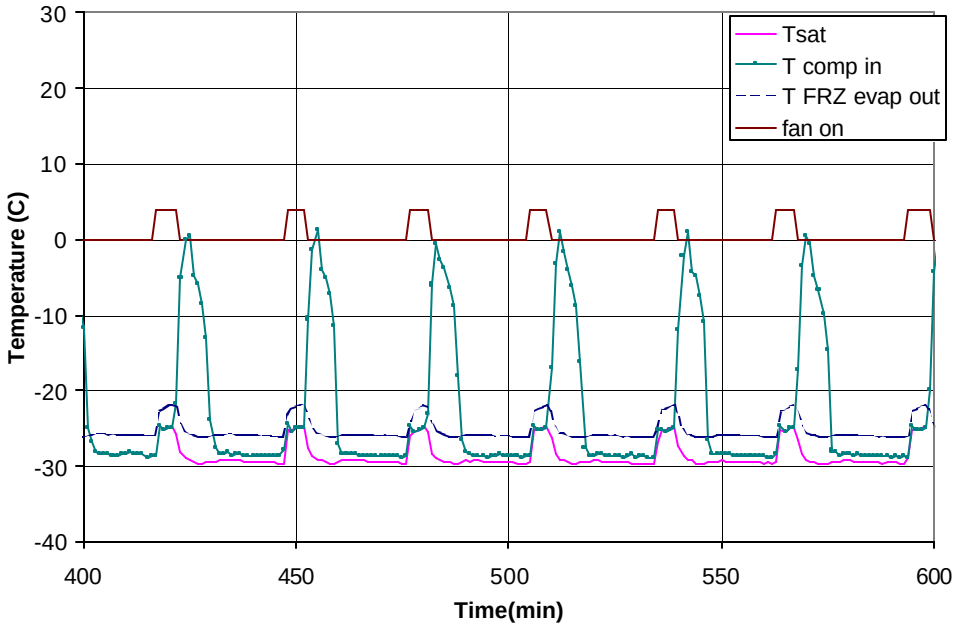

Figure E.2.1 Freezer Evaporator Exit and Compressor Inlet Refrigerant Conditions (350g Charge 16°C Ambient Temperature)

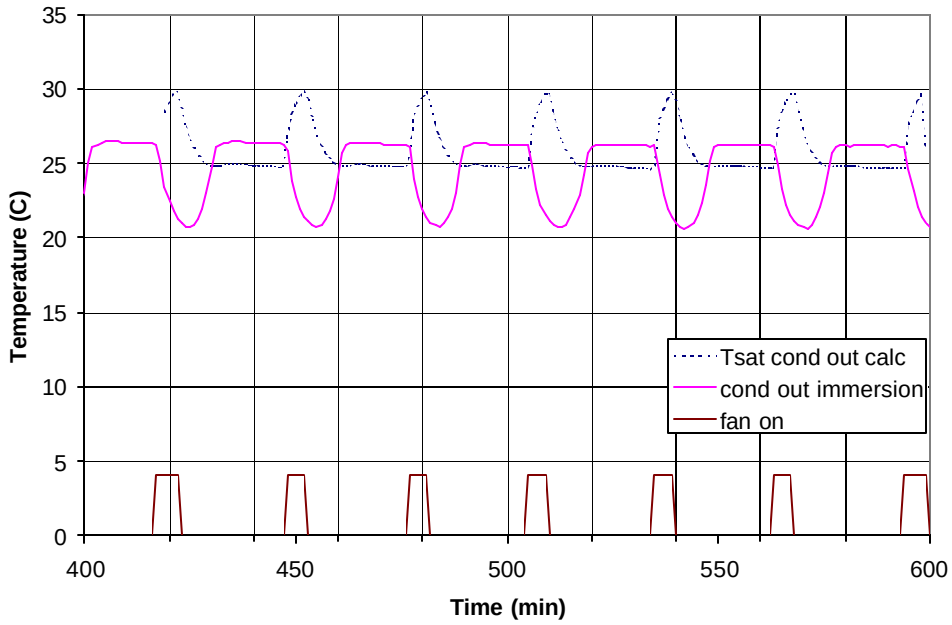

Figure E.2.2 Condenser Exit Refrigerant Conditions (350g Charge 16°C Ambient Temperature)

E.3 25°C Ambient Temperature 350 Gram Charge Test

In this test, the refrigerant enters the compressor as two-phase during the whole fan-on period. Again the fan-on periods are short enough that there is not enough time for the refrigerant accumulated in the fresh food evaporator to boil off and allow superheat at the compressor inlet. Superheat at the inlet starts as soon as the fan turns off and the evaporator pressure drops. As the fresh food evaporator refills, the superheat drops off and the refrigerant at the compressor inlet returns to two-phase about when the fan turns on. This timing appears to be coincidental and a factor of the separate processes of the fresh food compartment warming to the appropriate temperature to turn the fan on and the evaporator refilling.

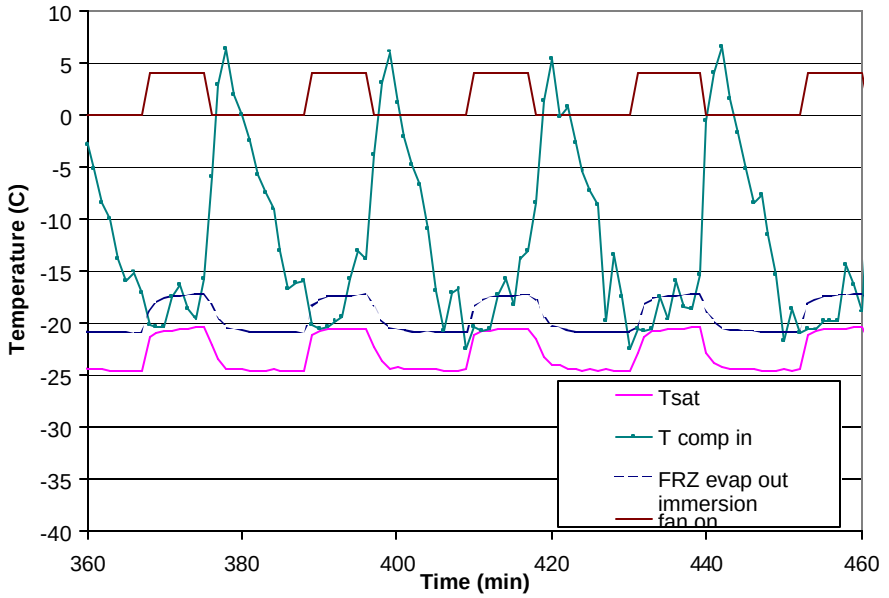

Figure E.3.1 Freezer Evaporator Exit and Compressor Inlet Refrigerant Conditions (350g Charge 25°C Ambient Temperature)

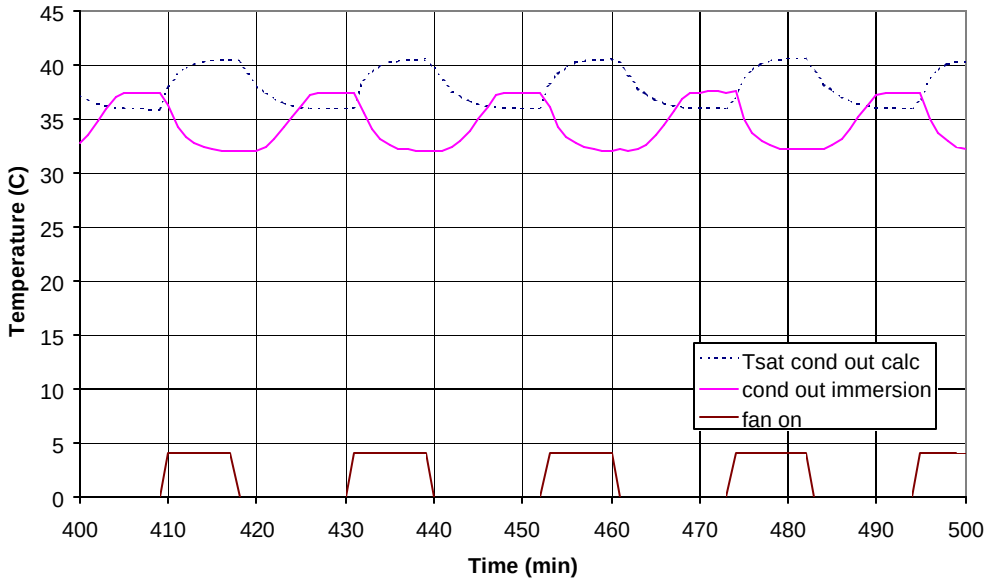

Figure E.3.2 Condenser Exit Refrigerant Conditions (350g Charge 25°C Ambient Temperature)